Supplementary data

TLR5 signaling amplifies airway epithelial cell responses to influenza through a MyD88–JAK1 crosstalk

Authors

Elaa Chkhaydem[1], Isabelle Fleurot[1], Iuliia Parfenova[2], Vanaique Guillory[1], Emmanuel Kut[1], Celine Barc[3], Jérémy Pezant[3], Stefanie Ebersberger[4], Isabelle Seufert[4], Laetitia Gaigeard[5], Marie Couralet[5], Gaëlle Simon[6], Pascal Barbry[5,7,8], Jean-Claude Sirard[9], Ferdinand Roesch[1], Sascha Trapp[1], Ignacio Caballero[1,10,*].

Affiliations

[1]Infectiologie et Santé Publique, UMR1282, INRAE, University of Tours, 37380 Nouzilly, France.
[2]d-fine AG, Zurich, Switzerland.
[3]INRAE, UE1277 PFIE, Nouzilly, France.
[4]d-fine GmbH, Frankfurt am Main, Germany.
[5]Université Côte d'Azur, CNRS, INSERM, Institut de Pharmacologie Moléculaire et Cellulaire, 06560 Sophia Antipolis, France.
[6]Swine Virology, Innovation and Genomics Unit, Ploufragan-Plouzané-Niort Laboratory, French Agency for Food, Environmental and Occupational Health and Safety (ANSES), Ploufragan, France.
[7]3IA-Côte d'Azur, 06560 Sophia Antipolis, France.
[8]IHU Respirera, 06560 Sophia Antipolis, France.
[9]Univ. Lille, CNRS, INSERM, CHU Lille, Institut Pasteur de Lille, U1019 – UMR9017 - CIIL - Center for Infection and Immunity of Lille, F-59000 Lille, France.
[10]Toxalim, Université de Toulouse, INRAE, ENVT, EI-Purpan, Toulouse, France.

***Corresponding author:** ignacio.caballero-posadas@inrae.fr

Supplementary Material and Methods

Cell lines

The T3 cell line was generated from primary porcine bronchial epithelial cells using a functional immortalization approach, as described in López-Gálvez et al. 2021[1]. Cells were maintained at 37°C and 5% CO_2 in supplemented huAEC medium with supplement (Inscreenex, IN-ME-1013BS) containing 1% penicillin-streptomycin (Invitrogen). For experimental procedures, cells were seeded onto collagen-coated plates.

Reagents and chemical inhibitors

Recombinant porcine IFN-α (171051) was purchased from PBL Assay Science (USA). Stock solutions of pharmacological inhibitors, BAY 11-7082 (B5556-10MG; Sigma-Aldrich) and JAK Inhibitor I (420099-500UG; Millipore), were prepared such that the final concentration of DMSO in the culture medium remained below 0.1%. Working concentrations of 10 µM JAK Inhibitor I and 5 µM BAY 11-7082 were applied continuously to T3 cells throughout the experiment. Primary antibodies and their corresponding dilutions were as follows: rabbit anti-STAT2 antibody (1:200; 72604, Cell Signaling Technology); mouse anti-IFNAR1 (1:200; 16-5945-85, Thermo Fisher Scientific); mouse anti-MyD88 (1:400; clone B-1, sc-136970, Santa Cruz Biotechnology); rabbit anti-JAK1 (1:400; clone 6G4, #3344, Cell Signaling Technology); rabbit anti-P65 (1:200; D14E12, Santa Cruz Biotechnology). Secondary antibodies conjugated to fluorophores used for immunofluorescence (1:1000) are Alexa Fluor 594 goat anti-rabbit (A11012, Thermo Fisher Scientific), Alexa Fluor 488 goat anti-mouse IgG (A11029, Thermo Fisher Scientific), and Alexa Fluor 647 goat anti-mouse (A21236, Thermo Fisher Scientific). HRP-conjugated secondary antibodies used for Western blotting (1:5000) were goat anti-mouse IgG (31444, Invitrogen) and goat anti-rabbit IgG (31460, Invitrogen).

Cell viability assay

Cell viability following treatment with BAY 11-7082 and JAK Inhibitor I was evaluated using the CytoTox-Glo™ Cytotoxicity Assay (G9290, Promega). T3 cells (2×10^5) were plated in 24-well plates and exposed to the inhibitors for 48 h before measurement. Luminescence was measured on a GloMax microplate reader.

Production of recombinant flagellin

The recombinant flagellin used in this study, *i.e.* FLAMOD (recombinant flagellin $FliC_{\Delta 174\text{-}400}$ harboring one additional N-terminal amino acid) is derived from *Salmonella enterica* serovar Typhimurium FliC[2,3] and was produced as described previously[1,2,4]. The recombinant flagellin $FliC_{\Delta 174\text{-}400}$ lacks the antigenic domain of native flagellin. This truncated molecule has a lower intrinsic antigenicity, compared to native flagellin, and it has been demonstrated to be safe following repeated flagellin administrations. The flagellin was purified by filtration and chromatography and resuspended in UltraPure™ DNase/RNase-Free Distilled Water (Thermo Fisher Scientific). FLAMOD was verified to be immunologically active in TLR5 reporter cells and in mouse-based assays. The endotoxin content was < 14 endotoxin units per mg of FLAMOD, as determined by the Limulus amebocyte lysate assay

The mutated flagellin variant, $FliC_{\Delta 174–400/89–96*/6H}$, (referred to as $FliC_{\Delta 3.1}$), was generated by site-directed mutagenesis of a plasmid encoding the truncated *Salmonella enterica* serovar Typhimurium and biologically active $FliC_{\Delta 174–400/6H}$ variant (referred to as $FliC_{\Delta 3}$). This modification replaced the TLR5-binding epitope (residues 89–96, QRVRELAV) with the corresponding sequence from *Helicobacter pylori* flagellin and introduced an N-terminal histidine tag. The resulting $FliC_{\Delta 3.1}$ variant is biologically inactive, as it fails to engage TLR5, as demonstrated by cell signaling assays and structure-based analysis[5–7].

Virus strain

The H3N2-Bissendorf03 strain (A/Swine/Bissendorf/IDT1864/2003), was isolated from a pig showing signs of acute respiratory disease and was kindly provided by Ralf Dürrwald, IDT Biologika GmbH (Dessau-Rosslau, Germany). The $H1_{av}N2$ strain (A/Swine/35-200154/2020; HA-1C.2.4), a representative of one of the most prevalent SIAV lineages in France since 2020[8,9], was kindly provided by the ANSES National Reference Laboratory for Swine Influenza (ANSES Ploufragan-Plouzané-Niort). Both strains were propagated in Madin-Darby canine kidney (MDCK) cells at a multiplicity of infection (MOI) of 0.001. After 48 h of incubation, supernatants were collected and stored at –80 °C. Viral titers were determined using the $TCID_{50}$ assay.

Viral Infection of T3 cells

Porcine bronchial epithelial T3 cells were seeded in collagen-coated sterile 24-well plates at a density of 2×10^5 cells per well and infected with the H3N2 or $H1_{av}N2$ virus at an MOI of 0.1. After 1 hour of incubation at 37°C with 5% CO_2 to allow viral adsorption, cells were washed once with Dulbecco's phosphate-buffered saline (PBS) (Sigma-Aldrich, D8537) to remove unbound virus and subsequently treated or not with 100 ng/mL of FLAMOD, $FliC_{\Delta 3}$ or $FliC_{\Delta 3.1}$ according to the experimental design.

Viral Titration by $TCID_{50}$

Viral titers were determined using 96-well plates seeded with MDCK cells at a density of 3.5×10^4 cells per well in Minimum Essential Medium (MEM) supplemented with 7.5% fetal bovine serum and 1% penicillin-streptomycin. Serial ten-fold dilutions of the virus were prepared in unsupplemented MEM containing TPCK-treated trypsin (1 µg/mL; LS003740, Worthington Biochemical) and added to the MDCK monolayers, with each dilution distributed across eight replicate wells. Cells were incubated at 37°C with 5% CO_2 for 72 hours and cytopathic effects (CPE) were assessed by crystal violet staining. The $TCID_{50}$ was calculated using the Reed-Muench method, expressing the viral concentration as the dilution causing cytopathic effects in 50% of the wells. Results are expressed as $TCID_{50}$/mL.

For titration of *in vivo* samples, a 250–300 mg fragment was cut from frozen OCT-embedded tissue (right cranial lobe) and excess OCT was removed manually. Tissue fragments were kept on dry ice throughout cutting to avoid thawing. Samples were transferred to tubes containing ceramic beads and homogenized at 20% (w/v) in MEM using a Precellys 24 homogenizer. Homogenates were clarified by centrifugation (2,000 g, 15 min, 4 °C) and ten-fold serial dilutions of the supernatant were prepared in MEM containing TPCK-treated trypsin (1 µg/mL). MDCK cells in 96-well plates were inoculated

with 100 µL of each dilution and incubated for 1 h at 37 °C with 5% CO_2 to allow viral adsorption. The inoculum was then removed, cells were washed once with MEM, and fresh MEM containing TPCK-treated trypsin (1 µg/mL) was added. Plates were incubated for 3 days at 37 °C with 5% CO_2 and CPE was assessed by crystal violet staining. The $TCID_{50}$ was calculated by the Reed-Muench method and titers are expressed as $\log_{10}$ $TCID_{50}$ per gram of lung tissue.

Immunofluorescence and image analysis

After stimulation, T3 cells were fixed in 4% paraformaldehyde for 20 min, washed with PBS-glycine (0.1 M), permeabilized with PBS 0.1% Triton X-100 for 15min and blocked with PBS 2% BSA for 1h. Cells were stained with the corresponding primary antibodies diluted in PBS 1% BSA and incubated overnight at 4°C. After three washes with PBS, cells were incubated with the appropriate secondary antibodies for 1h at room temperature. Nuclei were stained with 500 ng/ml of DAPI in PBS for 15 min. Samples were imaged using a Leica TCS SP8 confocal microscope with the Leica Application Suite AF software. Cellpose[10] was used to segment the cytoplasm and nuclei segmentation and the resulting masks were imported into Cellprofiler v4.2.6[11] for quantification of mean and total fluorescence intensity.

RNA Extraction and Quantitative PCR (RT-qPCR)

Total RNA was isolated using the RNA XS Plus kit (740990.5, Macherey-Nagel) according to the manufacturer's protocol. Briefly, 200 ng of total RNA was reverse transcribed using the iScript Reverse Transcription Supermix (1708841, Bio-Rad) in a T100 Thermal Cycler (Bio-Rad) under the following conditions: 5 min at 25 °C, 20 min at 46 °C, and 1 min at 95 °C. The resulting cDNA was subsequently used as a template for PCR performed with the Takyon No Rox SYBR MasterMix blue dTTP (UF-NSMTB0701, Eurogentec) on a CFX Thermal Cycler (Bio-Rad). The amplification program consisted of an initial denaturation step at 95 °C for 3 min, followed by 40 cycles of 95 °C for 10 s, and 60 °C for 4 s. A melting-curve analysis was then performed from 58 °C to 65 °C, with 1 °C increments every 0.1 min, to verify amplification specificity.

Samples were normalized using the mean cycle quantification (Cq) values of three endogenous reference genes: beta-2-microglobulin (B2M), glyceraldehyde-3-phosphate dehydrogenase (GAPDH), and ribosomal protein L19 (RPL19). Relative gene expression levels were calculated using the ΔΔCq method, compared to the negative control of each experiment. Primers are described in Supplementary Table 1

Microfluidic RT-qPCR

Total RNA was isolated using the RNA XS Plus kit as described above. cDNA was synthesized from 20 ng of RNA using the iScript Reverse Transcription Supermix (1708841, Bio-Rad). Pre-amplification was performed on cDNA diluted 1:10 in RNase-free water using the Preamp Master Mix (100-5581, Fluidigm) in a T100 thermal cycler (Bio-Rad). Each reaction contained 1 µl of Preamp Master Mix, 0.5 µl of 500 nM primer stock, 2.25 µl of water, and 1.25 µl of diluted cDNA. Primers were designed with an annealing temperature of 60°C and validated for efficiency, linearity, and specificity. Pre-amplification was carried out with an initial step at 95°C for 2 minutes, followed by 14 cycles of 95°C for 15 seconds and 60°C for 4 minutes. Pre-amplified cDNA was treated

with Exonuclease I (MO293, New England Biolabs) for 30 minutes at 37°C, followed by 15 minutes at 80°C, and then diluted 1:5 in TE buffer (10 mM Tris-HCl, 1.0 mM EDTA, pH 8.0).

RT-qPCR was performed in a 96x96 Dynamic Array Integrated Fluidic Circuits (Fluidigm), combining 96 samples with 96 primer sets, yielding 9216 simultaneous reactions. For each sample, the reaction mix contained 3 µl of 2X SsoFast EvaGreen with Low Rox (172-5211, Biorad), 0.3 µl of 20X DNA binding dye (100-7609, Fluidigm), and 2.7 µl of pre-amplified cDNA. Primer mixes for each of the primer sets were: 3.5 µl of 2x assay loading reagent (Fluidigm), 2.8 µl of TE (10 mM Tris, 0.1 mM EDTA, pH 8.0), 0.35 µl of 100 µM forward primer and 0.35 µl of 100 µM reverse primer. Five microliters of the reaction mix and primer mix were dispensed into the appropriate inlets and loaded into the circuit.The thermal cycle conditions were 1 minute at 95°C, followed by 30 cycles of 5 seconds denaturation at 96°C and 20 seconds annealing/extension at 60°C. Data were analyzed using the ΔΔCt method, normalizing target gene expression to two reference genes (GAPDH and RPL19). Results are expressed as relative fold changes (FC) compared to a control consisting of non-infected and untreated samples.

Generation of CRISPR/Cas9 knock-out (KO) cell lines

Single guide RNAs (sgRNAs) were designed to specifically disrupt the IFNAR1, TRAF6 and MyD88 *loci* (Supplementary Table 2) and were synthesized by Thermo Fisher Scientific. A matched set of three non-targeting control sgRNAs (AAAACAGGACGAUGUGCGGC, AAAACAUCGAAGCGU, and AAAAUAGCAGUAAACUCAAC) directed against non-genomic sequences was used to generate negative control cell lines. All sgRNAs were supplied by Thermo Fisher Scientific and used at a concentration of 20 pmol/µL. The sgRNAs (12 pmol) were separately complexed with 2µg of TrueCut Cas9 Protein v2 (A36499, Thermo Fisher). Ribonucleoprotein (RNP) complexes were incubated at room temperature for 10 minutes prior to use.

T3 cells were detached, washed with PBS, and resuspended in Resuspension Buffer R (MPK1096R, Thermo Fisher Scientific) at a concentration of 2×10^5 cells per 5 µL. Cells were electroporated with the Cas9/sgRNA ribonucleoprotein complexes using the Neon Transfection System (Thermo Fisher Scientific) under the following conditions: 10 µL tip, 1200 V, 20 ms with 4 pulses. Electroporated cells were immediately transferred to pre-warmed huAEC growth medium with supplements and without antibiotics. Four days post-electroporation, cells were harvested for genomic DNA extraction.

Genomic DNA was isolated using the NucleoSpin® Tissue kit (740952, Macherey-Nagel) according to the manufacturer's instructions. PCR amplicons encompassing the target sites were generated using Q5® Hot Start High-Fidelity DNA Polymerase (M0493, NEB). Primer sequences are listed in Supplementary Table 3.

PCR cycling conditions were 98°C for 30 s followed by 35 cycles of 98°C for 10 s, 65°C for 30 s, and 72°C for 60 s, with a final extension at 72°C for 2 min. PCR products were purified using the Gel and PCR Clean-up Kit (740608, Macherey-Nagel™) and submitted for Sanger sequencing at Eurofins Genomics. Insertions and deletions (indels) were quantified using the ICE analysis tool (https://ice.synthego.com/#/, Synthego).

Protein expression of IFNAR1 and MyD88 was evaluated by confocal microscopy in knockout and negative control cells two weeks after electroporation. Functional validation of the *IFNAR1* knockout was performed by stimulating *IFNAR1* knockout and negative control cells with 10 U/mL porcine IFN-α (171051, PBL Assay Science) for 30 min, followed by assessment of STAT2 nuclear translocation by confocal microscopy, as described above. Functional validation of the *TRAF6* knockout was performed in parallel by stimulating *TRAF6* knockout and negative control cells with 100 ng/mL FLAMOD for 40 min, followed by evaluation of NF-κB p65 nuclear translocation by confocal microscopy.

Co-immunoprecipitation and Western blotting

T3 cells were seeded in 6-well plates at a density of 1 × 10^6 cells per well. The following day, cells were stimulated with porcine IFN-α (10 UI/ml) for 30 min in the presence or absence of 100 ng/ml of FLAMOD. Cells were lysed in 150 µL of IP lysis buffer (Cat. No. 87788, Thermo Fisher Scientific) supplemented with protease and phosphatase inhibitors (Cell Signaling Technology, Cat. No. 5872S) and incubated on ice for 30 min with intermittent mixing. Lysates were clarified by centrifugation at 13,000 × g for 15 min at 4 °C. Ten percent of each lysate was set aside as input control; the remaining 90% was incubated overnight at 4 °C with 0.5 µg of mouse monoclonal anti-MyD88 antibody (clone B-1, Santa Cruz Biotechnology, sc-136970). Before use, 30 µL of Protein G–Sepharose beads (GE17-0618-01, Cytiva) were washed three times in lysis buffer and recovered after each wash by centrifugation at 2,000 × g for 2 min at 4 °C. The washed beads were then added to the antibody–lysate mixture and incubated for 4 h at 4 °C under agitation. Beads were then collected by centrifugation at 5,000 × g for 2 min at 4 °C and washed three times with lysis buffer. Bound immunoprecipitated proteins were eluted in 30 µL of Laemmli buffer by gentle vortexing and incubation at 50 °C for 10 min, followed by a brief centrifugation at maximum speed.

Immunoprecipitated proteins and input samples were resolved by SDS–PAGE on precast polyacrylamide gels (Mini-PROTEAN TGX, Bio-Rad, Cat. No. 4569033) and transferred onto nitrocellulose membranes using a semi-dry system (Trans-Blot Turbo, Bio-Rad). Membranes were blocked for 1 h at room temperature in TBS containing 5% BSA (Sigma-Aldrich, Cat. No. A7906) and then incubated overnight at 4 °C with primary antibodies diluted in blocking buffer: mouse monoclonal anti-MyD88 (1:400, clone B-1, Santa Cruz Biotechnology, sc-136970) and rabbit monoclonal anti-JAK1 (1:400, clone 6G4, Cell Signaling Technology, Cat. No. 3344). After washing with TBS, membranes were incubated for 1.5 h at room temperature with HRP-conjugated secondary antibodies (1:5000): goat anti-mouse IgG (Invitrogen, Cat. No. 31444) and goat anti-rabbit IgG (Invitrogen, Cat. No. 31460). Bands were detected using an enhanced chemiluminescence substrate (Immobilon Western HRP Substrate, MilliporeSigma, Cat. No. WBKLS0500).

Animals and ethical statement

In vivo experiments were performed at the INRAE-PFIE platform (Plateforme d'Infectiologie Expérimentale, UE-1277, INRAE Centre Val de Loire, France). A total of 15 healthy 4-week-old large white pigs were obtained from the EUPAO experimental herd (Unité Expérimentale de Physiologie Animale de l'Orfrasière, UE1297 UEPAO, INRAE,

Centre Val de Loire, France). Pigs were screened on arrival and confirmed seronegative for swine influenza A virus. Animals were kept in Biosafety Level 2 confined housing (9 m²/pig) that was cleaned daily throughout the experimental procedure. Pigs had access to a standard grain-based diet (Sanders) and water *ad libitum*, and social and material (balls) enrichment was provided to support animal welfare. Physical condition and welfare were monitored as previously described[1]. Pigs were anesthetized to minimize pain and distress during inoculation with either FLAMOD or SIAV as described in[1]. For sacrifice, pigs were anesthetized as above, administered i.v. heparin (Choay®, 25 000 UI/5 mL; Sanofi-Adventis, France), and exsanguinated prior to post-mortem sampling.

All experiments were conducted in accordance with the guidelines of the Institutional Animal Care and Use Committee at INRAE. All experimental procedures were evaluated by the local ethics committee (Comité d'éthique en expérimentation animale Val de Loire, CEEA) and approved by the Ministry of Higher Education and Research (APAFIS #43578-2023051616364291).

Pig SIAV infection and FLAMOD treatment

Pigs were randomly allocated to three experimental groups, balanced for sex: mock-infected controls (n = 3; 1 female, 2 males), $H1_{av}N2$-infected pigs treated with vehicle (NaPi buffer; n = 6; 3 females, 3 males), and $H1_{av}N2$-infected pigs treated with FLAMOD (n = 6; 3 females, 3 males).

Animals were anesthetized and inoculated via the intratracheal route with 2×10^6 $TCID_{50}$ of the $H1_{av}N2$ in a total volume of 2 mL of sterile PBS using an esophageal probe. Mock-infected controls received an equivalent volume of sterile PBS via the same route. One hour after viral inoculation, infected pigs received either 1.3 mg of FLAMOD or an equivalent volume of NaPi buffer by intratracheal aerosol administration using an Aerogen mesh nebulizer system. Animals were monitored daily following inoculation to assess infection, disease progression and discomfort. Humane endpoints were predefined to avoid unnecessary animal suffering that required euthanasia.

Clinical scoring

Animals were monitored twice daily over the 72-hour observation period by trained observers blinded to treatment allocation. Clinical signs were recorded as binary events (present/absent) and included increased respiratory frequency, irregular breathing, cough, lethargy and reduced mobility. The clinical score for each animal at each time point was defined as the sum of all observed signs (range 0–5), and the cumulative clinical score was calculated as the sum of all scores across the entire observation period.

ELISA

Serum samples were collected before treatment (0 hours), at 24 hours post-inoculation and immediately before sacrifice (72 hours post-infection). The acute phase protein C-reactive protein (CRP) was quantified in serum using a Pig CRP ELISA Kit (NBP2-67253, Bio-Techne) in accordance with the manufacturer's instructions.

Pig lungs snRNA-seq - Sample preparation

Lung tissue samples were collected from the right cranial lobe, at the first lobar bronchial bifurcation, embedded in OCT compound, frozen on dry ice and stored at −80 °C.

Adjacent tissue sections from the same block were used for both single nuclei RNA sequencing (snRNA-seq) and viral titration. Nuclei were isolated as previously described[12]. Briefly, 300 µm cryosections of OCT-embedded lung tissue were homogenized into a pre-chilled glass Dounce homogenizer containing 1 mL of citric acid–sucrose buffer (0.25 M sucrose, 25 mM citric acid). The tissue underwent multiple homogenization steps (loose- and tight-pestle strokes) with incubation on ice, followed by filtration through a 40 µm cell strainer. The strainer was rinsed with an additional 1 mL of citric acid–sucrose buffer. After centrifugation (500 × g, 5 min, 4 °C), the pellet was resuspended in 1 mL of wash buffer (10 mM Tris-HCl pH 7.4, 10 mM NaCl, 3 mM $MgCl_2$, 1% BSA, 0.1% Tween-20, 1 mM DTT, 0.4 U/µL RNaseIn, 0.4 U/µL riboblock), passed through a 5 µm cell strainer and centrifuged again. Nuclei were resuspended in 300 µL of cold PBSA-BSA (1.5%). Nuclei morphology and concentration were assessed manually on a hemocytometer. RNA integrity was assessed on an Agilent Bioanalyzer system prior to library preparation. snRNA-seq libraries were prepared using the Chromium GEM-X Single Cell 3' reagent kit v4 according to the manufacturer's protocol with a target capture of 20000 nuclei per sample and sequenced on Illumina NextSeq 2000.

Single-cell RNA-seq data processing and cell type annotation

Raw sequencing reads were aligned to a combined reference comprising the Sus scrofa Sscrofa11.1 pig genome and the eight genomic segments of A/swine/France/35-200154/2020 (H1N2 strain; GenBank accessions MZ088854–MZ088861) using Cell Ranger v9.0.1 (10x Genomics), generating per-sample gene expression matrices. Doublet identification and donor demultiplexing were performed using Demuxafy v3.0.0, which integrated five independent tools (DoubletFinder, scds, scDblFinder, Souporcell, and Vireo). Genotype-based methods (Souporcell and Vireo) used common SNPs overlapping genes with minor allele frequency >5%. Outputs were integrated using Demuxafy's majority-vote method ("MajoritySinglet"), and droplets classified as singlets with a confirmed donor assignment were retained for downstream analysis.

Ambient RNA was estimated and removed using decontX (celda R package v1.26.0). Nuclei in the bottom and top 5th percentiles of detected genes (nFeature_RNA) and nuclei with mitochondrial transcript fraction ≥5% of total UMI (unique molecular identifier) counts were excluded. In addition, a small cluster of 100 cells exhibiting multi-lineage marker co-expression, likely residual doublets, was removed. After filtering, 135,349 cells were retained (79.5% of called droplets) for downstream analysis.

Downstream analysis was performed using Seurat v5.4.0. Counts were normalized using SCTransform, and PCA was performed on the top 3,000 most variable host genes (excluding viral genes). The PCA embedding served as input for CCA-based integration across samples, and the resulting 30-dimensional integrated embedding was used to construct the SNN graph and compute the UMAP. Clusters were identified using the Louvain algorithm at resolution 0.6. Cell clusters were annotated according to canonical gene markers: AT1 (*AGER, HOPX, RTKN2*), AT2 (*SFTPC, SFTPB, SFTPA1, LAMP3*), basal (*TP63, KRT5*), multiciliated (*FOXJ1, DNAH5, TPPP3*), club (*SCGB1A1, SCGB3A2*), tuft (*POU2F3, SH2D6, TRPM5, AVIL*), aerocyte (*PECAM1, CA4, EDNRB, HPGD*), general capillary (*GPIHBP1, PECAM1, EDNRB, APLNR*), arterial endothelial (*GJA5, BMX*), venous endothelial (*ACKR1, SELP, VWF*), lymphatic endothelial (*PROX1,*

MMRN1, CCL21), alveolar fibroblast (*TCF21, WNT2, GPC3*), adventitial fibroblast (*PI16, MFAP5, SCARA5*), pericyte (*TRPC6*,*NOTCH3, PDGFRB*), smooth muscle (*ACTA2, MYH11, CNN1, DES*), mesothelial (*WT1, UPK3B*), alveolar macrophage (*MARCO, CD163*), monocyte-derived macrophage (*CD163, VCAN, FCN1, F13A1, FCGR3A*), activated interstitial macrophage (*CD163, MRC1, DUOX2, CD9, LYZ*), quiescent interstitial macrophage (*CD163, MRC1, SELENOP*), cDC1 (*FLT3, ZBTB46, IRF8*), pDC (*FLT3, TCF4, IL3RA, IRF7, IRF8, BCL11A*), mast cell (*KIT, MS4A2*), naive T cell (*CD3E, CD4, CCR7, LEF1, TCF7, IL7R, SELL*), cytotoxic T cell (*CD3E, CD8A, CD8B, GZMB, GNLY, NKG7*), γδ T cell (*CD3E, SOX13, BLK*), proliferating lymphocyte (*CD3E, MKI67, TOP2A*), NK cell (*NCR1, KLRG1, KLRK1, NKG7, GNLY*), B cell (*MS4A1, CD79B*), plasma cell (*JCHAIN, MZB1, XBP1*).

Type I IFN and ISG module scoring

Module scores for type I IFN expression and type I and type II ISG responses were computed at the single-cell level using Seurat v5 AddModuleScore function on log-normalized expression data. The type I IFN gene panel comprised pig *IFN-α, IFN-ω, and IFN-δ* paralogs together with *IFNB1, IFNE, and IFNK*. Type I and type II interferon-stimulated gene (ISG) scores were computed using genes from the Molecular Signatures Database (MSigDB) Hallmark Interferon Alpha and Interferon Gamma gene sets (msigdbr R package v26.1.0), restricted to genes present in the dataset.

Pseudobulk meta-analysis of ISG module scores

To compare type I and type II ISG scores between FLAMOD- and NaPi-treated animals across all cell types, a two-stage pseudobulk random-effects meta-analysis was performed. Animals from the control group were excluded, retaining only $H1_{av}N2$-infected individuals receiving either NaPi (n = 6) or FLAMOD (n = 6) treatment. Prior to analysis, cells were stratified by infection state (bystander, low, high viral load).

In the first stage, donor-level pseudobulk means of ISG scores were computed per cell type, per animal, and per treatment group, requiring a minimum of three donors per group per cell type. The effect size for each cell type was defined as the mean difference in ISG score (FLAMOD minus NaPi), with standard error estimated by error propagation from donor-level standard deviations. In the second stage, cell-type-level effect sizes were pooled using restricted maximum likelihood (REML) random-effects meta-analysis implemented in the *metafor* package. Heterogeneity was quantified by I^2. A sign test (exact binomial, one-sided) was applied to assess whether the direction of effect was consistent across cell types beyond chance.

Pseudobulk differential expression gene (DEG) analysis

DEG analysis was restricted to bystander and cells with low viral loads due to the limited number of cell types represented per animal in the high viral load group. Comparisons were made between $H1_{av}N2$ + FLAMOD and $H1_{av}N2$ + NaPi animals (n = 6 per group). Pseudobulk profiles were generated by summing raw counts per animal per cell type using AggregateExpression in Seurat v5. Cell types were tested only when both treatment groups contributed more than 2 pseudobulk samples. Genes detected in fewer than 2 samples (counts < 10) were filtered prior to testing. Differential expression between

FLAMOD- and NaPi-treated animals was modeled with DESeq2. Significance was defined as FDR < 0.05.

Gene set enrichment analysis

Gene set enrichment analysis (GSEA) was performed independently for each cell type and infection state. Genes were ranked by their DESeq2 Wald statistic from the pseudobulk DEG analysis, and the ranked list was tested for enrichment of type I and type II ISGs retrieved as described above. Pre-ranked GSEA was performed using fgseaMultilevel from the fgsea R package (parameters: minSize = 10, maxSize = 500, eps = 0, nPermSimple = 10,000). Normalized enrichment scores (NES) were reported with Benjamini-Hochberg-adjusted p-values. Significance was defined as FDR < 0.05.

Statistics and Reproducibility

Statistical analyses were performed using R (version 4.4.3) and the packages ggplot2, ggpubr, rstatix, lmerTest, emmeans, drc, mclust, DESeq2, metafor and Seurat (RStudio, version 2026.4.0.526). Statistical details for each experiment, including the test used, exact sample size, and measures of dispersion and precision, are provided in the corresponding figure legends. Assumptions of normality and homogeneity of variance were evaluated prior to applying the appropriate statistical test. Student's *t*-test or the Mann–Whitney U test were used to measure the significance of the differences between two groups, depending on whether assumptions of normality were satisfied. Multiple groups were compared using one-way, two-way or three-way analysis of variance (ANOVA); for one-way designs, ANOVA was followed by Tukey's HSD post hoc test for pairwise comparisons. Knockout RT-qPCR experiments were analyzed using linear mixed-effects models with treatment, genotype and their interaction as fixed effects and experimental day as a random intercept. Longitudinal serum CRP concentrations were analyzed by a linear mixed-effects model on log-transformed values, with treatment, day and their interaction as fixed effects and pig as a random intercept. STAT2 nuclear-translocation dose-response curves were fitted to a four-parameter log-logistic model. For single-nucleus RNA-sequencing data, all inference was performed at the donor pseudobulk level using inverse-variance-weighted random-effects meta-analysis across cell types and DESeq2 for differential gene expression. The probability of error level (alpha) was set to 0.05. P values and the specific statistical test performed for each experiment are reported in the corresponding figure legends or main text. Unless otherwise stated, results are presented as individual data points with horizontal bars indicating the mean ± SEM.

References

1. López-Gálvez, R. *et al.* Airway Administration of Flagellin Regulates the Inflammatory Response to Pseudomonas aeruginosa. *Am J Respir Cell Mol Biol* **65**, 378–389 (2021).

2. Porte, R. *et al.* A Toll-Like Receptor 5 Agonist Improves the Efficacy of Antibiotics in Treatment of Primary and Influenza Virus-Associated Pneumococcal Mouse Infections. *Antimicrob Agents Chemother* **59**, 6064–6072 (2015).
3. Nempont, C. *et al.* Deletion of Flagellin's Hypervariable Region Abrogates Antibody-Mediated Neutralization and Systemic Activation of TLR5-Dependent Immunity. *The Journal of Immunology* **181**, 2036–2043 (2008).
4. Matarazzo, L. *et al.* Therapeutic Synergy Between Antibiotics and Pulmonary Toll-Like Receptor 5 Stimulation in Antibiotic-Sensitive or -Resistant Pneumonia. *Front. Immunol.* **10**, 723 (2019).
5. Andersen-Nissen, E. *et al.* Evasion of Toll-like receptor 5 by flagellated bacteria. *Proc. Natl. Acad. Sci. U.S.A.* **102**, 9247–9252 (2005).
6. Gewirtz, A. T. *et al. Helicobacter pylori* Flagellin Evades Toll-Like Receptor 5–Mediated Innate Immunity. *J INFECT DIS* **189**, 1914–1920 (2004).
7. Biedma, M. E. *et al.* Recombinant flagellins with deletions in domains D1, D2, and D3: Characterization as novel immunoadjuvants. *Vaccine* **37**, 652–663 (2019).
8. Deblanc, C. *et al.* Pathogenicity and escape to pre-existing immunity of a new genotype of swine influenza H1N2 virus that emerged in France in 2020. *Vet Res* **55**, 65 (2024).
9. Richard, G. *et al.* Major change in swine influenza virus diversity in France owing to emergence and widespread dissemination of a newly introduced H1N2 1C genotype in 2020. *Virus Evolution* **11**, veae112 (2025).
10. Stringer, C., Wang, T., Michaelos, M. & Pachitariu, M. Cellpose: a generalist algorithm for cellular segmentation. *Nat Methods* **18**, 100–106 (2021).

11. Stirling, D. R. *et al.* CellProfiler 4: improvements in speed, utility and usability. *BMC Bioinformatics* **22**, 433 (2021).
12. Caballero, I. *et al.* Cystic fibrosis alters the structure of the olfactory epithelium and the expression of olfactory receptors affecting odor perception. *Sci. Adv.* **11**, eads1568 (2025).

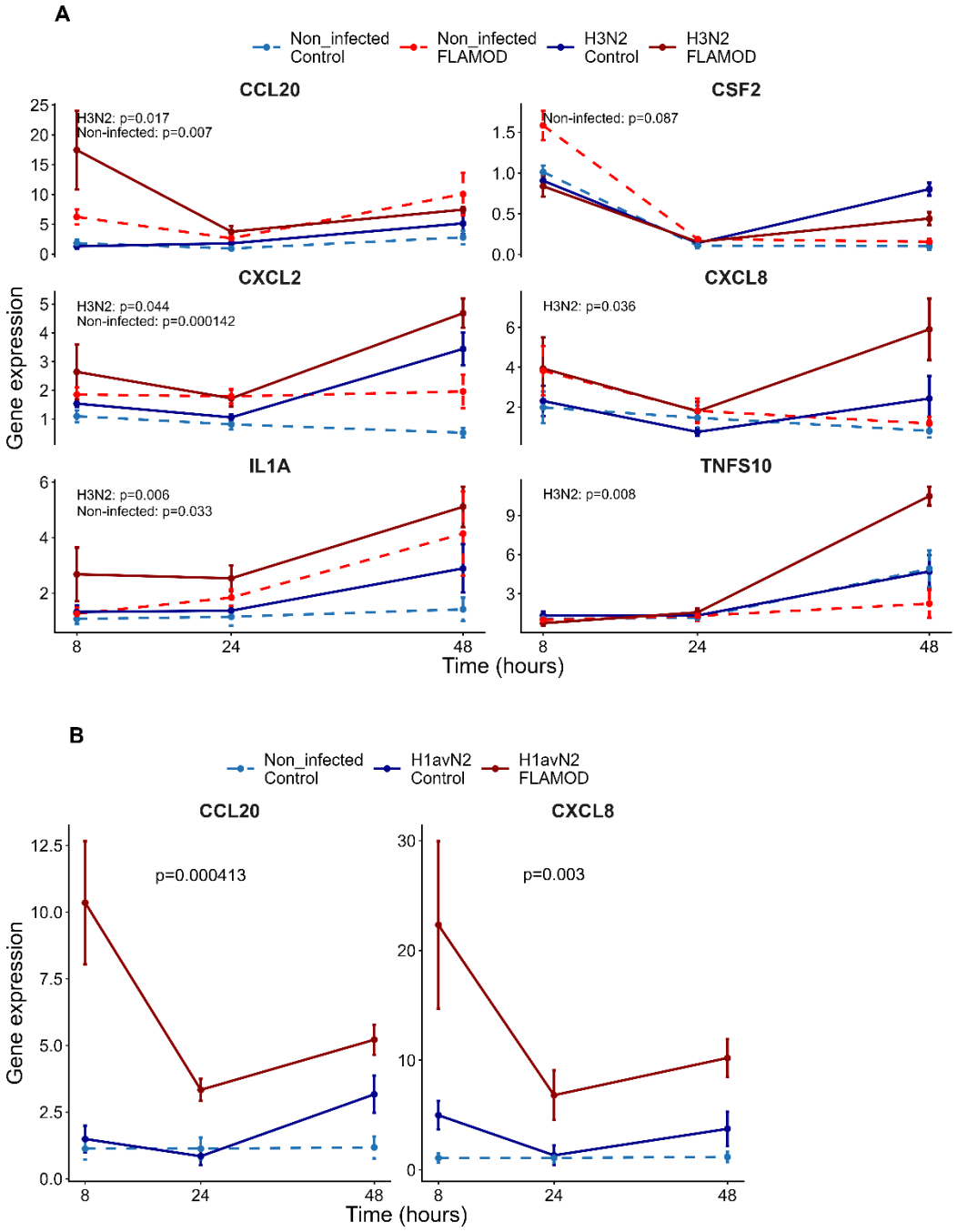


Fig. S1. Time-course expression cytokines in T3 cells infected or not with SIAV H3N2 (A) or SIAV H1avN2 (B) and treated or not with FLAMOD. Data are presented as mean fold change ± SEM (n = 6). p values indicate the main effect of FLAMOD treatment from a two-way ANOVA (FLAMOD × Time) within SIAV-infected cells. Dashed lines represent non-infected groups; solid lines represent SIAV-infected groups.

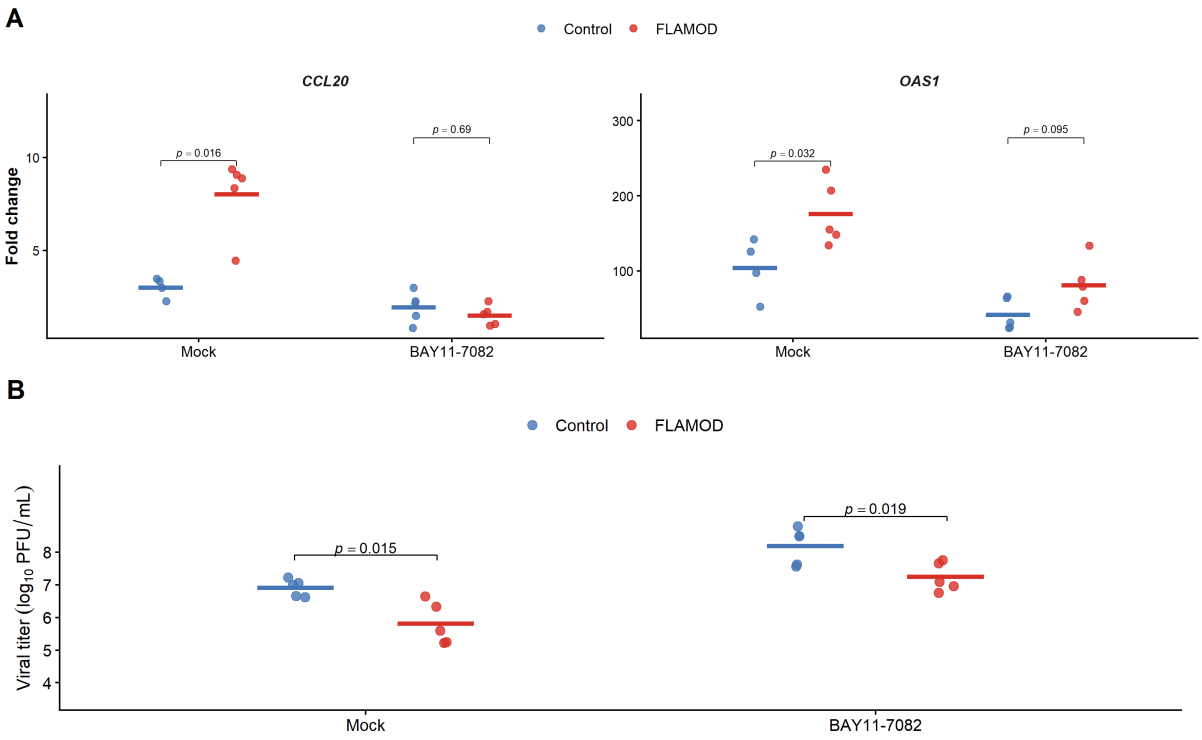


Fig. S2. FLAMOD-mediated antiviral response is not primarily dependent on the NF-κB pathway. T3 cells were infected with SIAV H3N2 and, 1 hour post-infection, treated with FLAMOD or left untreated, in the presence of either the NF-κB inhibitor BAY 11-7082 (5μM) or vehicle control (DMSO), for 48 hours. (A) *CCL20* and *OAS1* expression measured by RT-qPCR. Data are expressed as fold change relative to non-infected, untreated control. *p* values were calculated using the Mann-Whitney Wilcoxon test (n=4-5). (B) Viral titers at 48 hours post-infection determined by TCID50 assay on MDCK cells. *p* values were derived from two-sided Welch's t-tests comparing viral titers between Mock and FLAMOD-treated groups (n = 4–5). Each dot represents an individual biological replicate. Horizontal bars indicate the mean fold change.

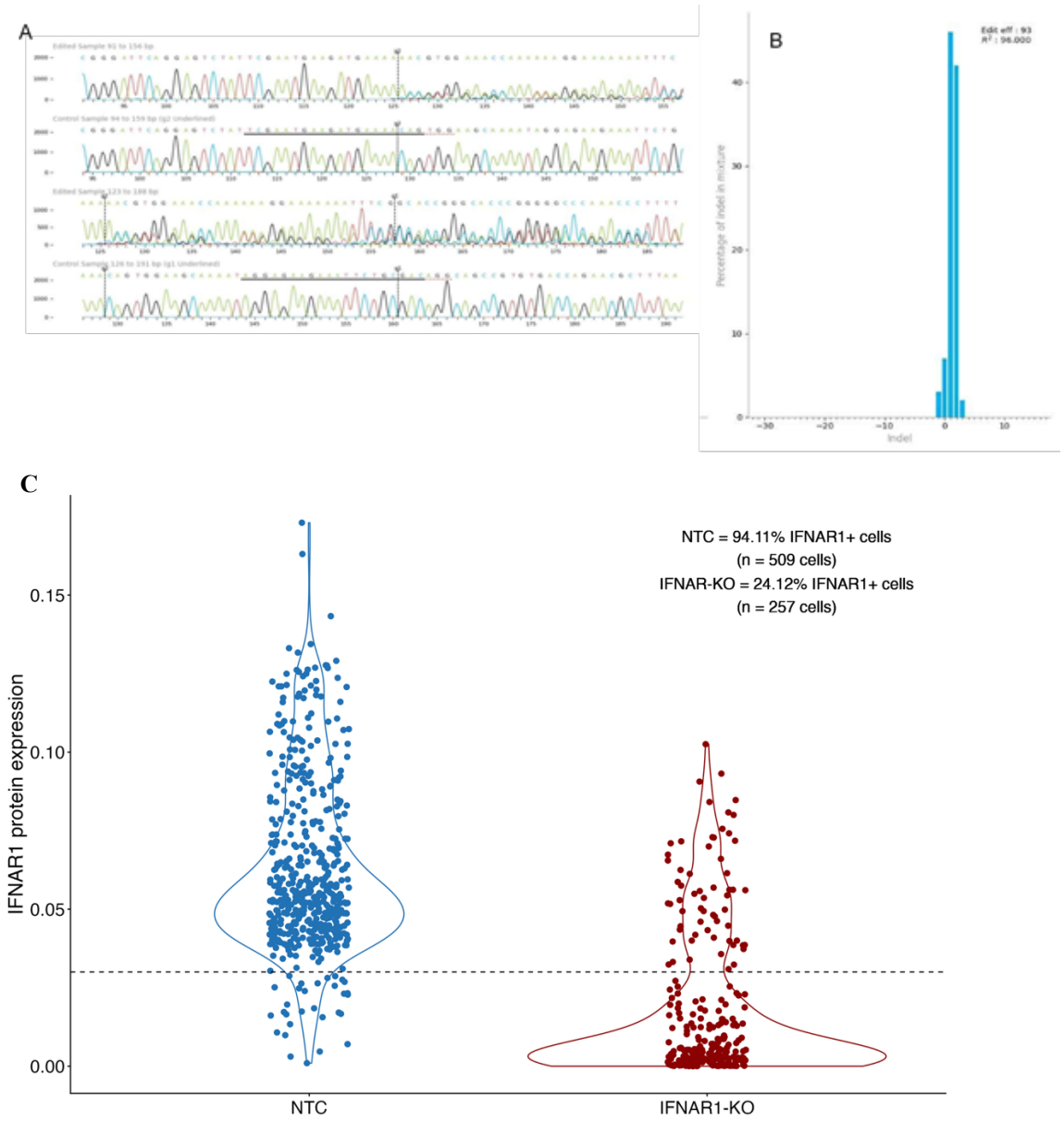


Fig. S3. ICE analysis of Sanger sequencing traces obtained for the IFNAR1 locus in negative control and CRISPR/Cas9-edited T3 cells. Genomic DNA was amplified across the sgRNA target region and the PCR products were analyzed by Sanger sequencing at Eurofins Genomics. Sequence traces were analyzed using the Synthego ICE (Inference of CRISPR Edits) web tool. The negative control (NTC) consisted of cells transfected with a non-targeting sgRNA designed not to recognize any genomic sequence. (A) Alignment of Sanger chromatograms covering the IFNAR1 sgRNA target site. In the negative control sample, the chromatogram remains clean and well resolved across the analyzed region, consistent with an unedited locus. In contrast, the edited sample shows overlapping and mixed peaks beginning at the expected Cas9 cleavage site, indicating the presence of a heterogeneous population of alleles carrying insertions and deletions (indels) generated by CRISPR/Cas9 system. The black

horizontal lines indicate the positions of the sgRNA target sequences (g1 and g2) within the IFNAR1 genomic region. (B) ICE-derived indel spectrum for the edited sample. The x-axis indicates indel size relative to the reference sequence, expressed in nucleotides, where negative values correspond to deletions, positive values to insertions. The y-axis represents the estimated proportion of each indel class within the cell population. ICE analysis estimated an overall editing efficiency of 93%, with a high coefficient of determination ($R^2 = 0.96$), supporting robust editing at the IFNAR1 locus. (C) Violin plot for IFNAR1 protein expression. The IFNAR1 positivity threshold (dashed line, 0.03) was defined as the intersection of the IFNAR1-KO and NTC cytoplasmic intensity distributions. The percentage of IFNAR1+ cells was calculated as the proportion of cells with a mean cytoplasmic IFNAR1 intensity above this threshold within each genotype (n = 509 WT cells; n = 257 KO cells).

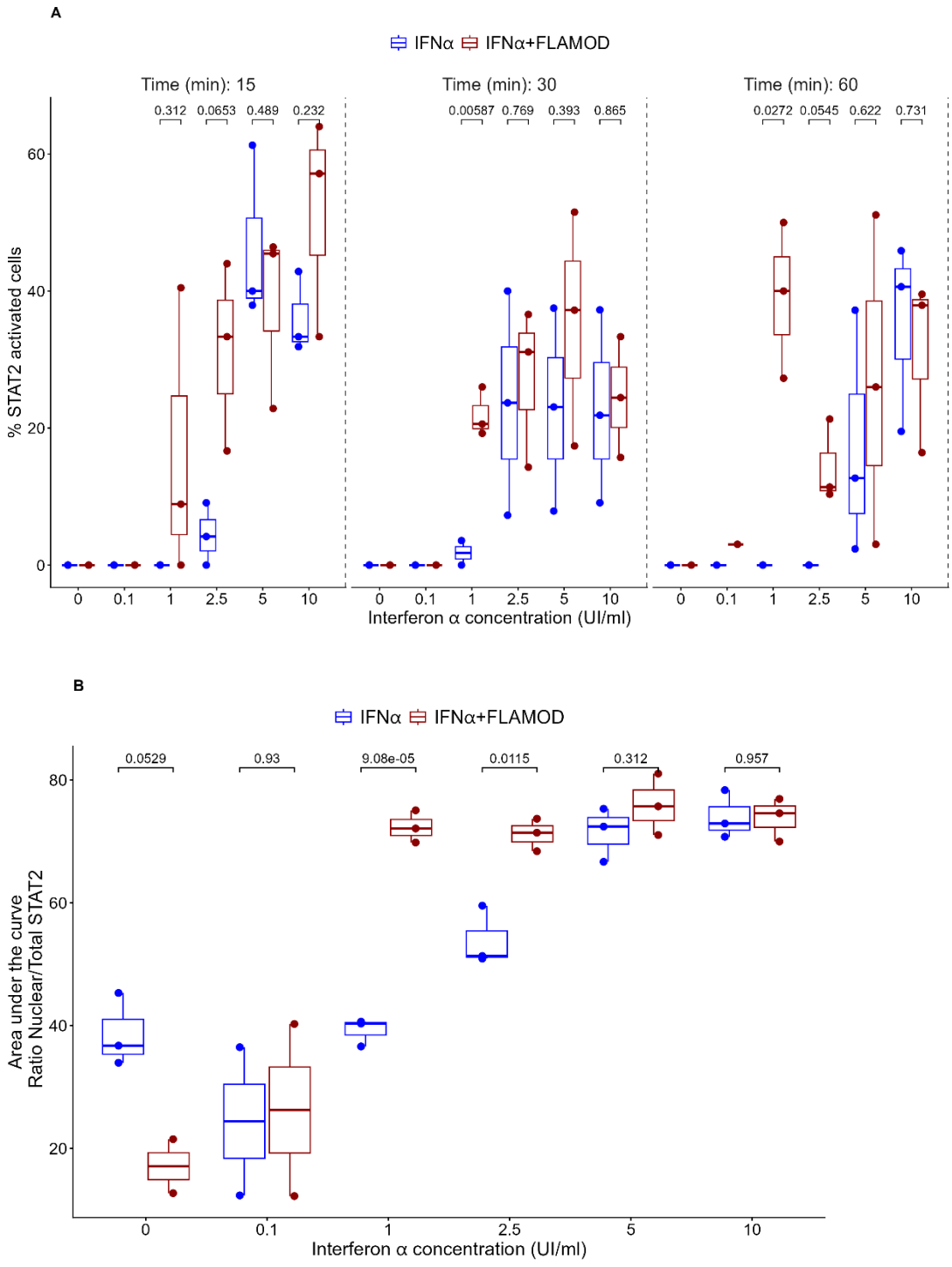


Fig. S4. FLAMOD increases the sensitivity of T3 cells to interferon-α. T3 cells were treated with FLAMOD (100 ng/mL) or left untreated and co-stimulated with increasing concentrations of interferon-α (IFN-α; 0–10 IU/mL) for 15, 30, or 60 min. (A) Percentage of STAT2-activated cells across IFN-α concentrations. Cells were scored as STAT2-activated when the nuclear/total STAT2 ratio exceeded a threshold defined as the mean + 2 standard deviations of unstimulated control

cells. Percentages were calculated per replicate. (B) Area under the curve (AUC) of the nuclear/total STAT2 ratio over time (trapezoidal method) for each IFN-α concentration. *p* values were derived from two-sided Welch's t-tests comparing IFN-α versus IFN-α + FLAMOD within each concentration. Individual dots represent independent replicates.

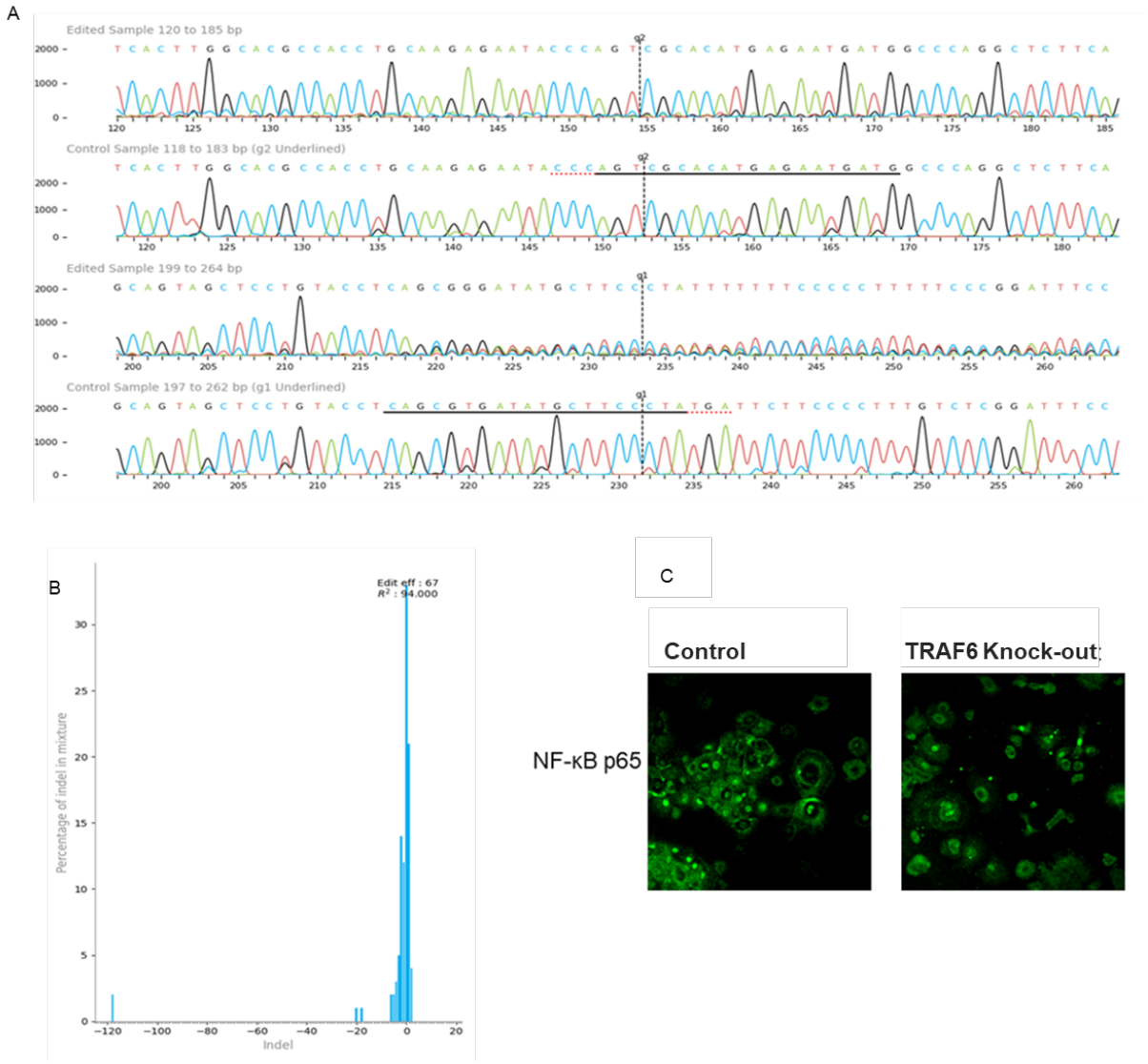


Fig. S5. Validation of TRAF6 knockout in CRISPR/Cas9-edited T3 cells. ICE analysis of Sanger sequencing traces obtained for the TRAF6 locus in negative control and CRISPR/Cas9-edited T3 cells. Genomic DNA was amplified across the sgRNA target region and the PCR products were analyzed by Sanger sequencing at Eurofins Genomics. Sequence traces were analyzed using the Synthego ICE (Inference of CRISPR Edits) web tool. The negative control (Control) consisted of cells transfected with a non-targeting sgRNA designed not to recognize any genomic sequence. (A) Alignment of Sanger chromatograms covering the TRAF6 sgRNA target site. In the negative control sample, the chromatogram remains clean and well resolved across the analyzed region, consistent with an unedited locus. In contrast, the edited sample shows overlapping and mixed peaks beginning at the expected Cas9 cleavage site, indicating the presence of a heterogeneous population of alleles carrying insertions and deletions (indels) generated by CRISPR/Cas9 system. The sequencing suggests that gRNA1 caused the stronger CRISPR editing. The black horizontal lines indicate the positions of

the sgRNA target sequences (g1 and g2) within the TRAF6 genomic region. (B) ICE-derived indel spectrum for the edited sample. The x-axis indicates indel size relative to the reference sequence, expressed in nucleotides, where negative values correspond to deletions, positive values to insertions. The y-axis represents the estimated proportion of each indel class within the cell population. ICE analysis estimated an overall editing efficiency of 67%, with a high coefficient of determination ($R^2 = 0.94$), supporting robust editing at the IFNAR1 locus. (C) Immunofluorescence staining of NF-κB p65 in control and TRAF6-KO T3 cells stimulated with FLAMOD (100 ng/mL) for 40 min. TRAF6-KO cells show impaired p65 nuclear translocation upon 30 min of FLAMOD stimulation confirming functional disruption of TRAF6-dependent NF-κB signaling. Green, anti-p65 .

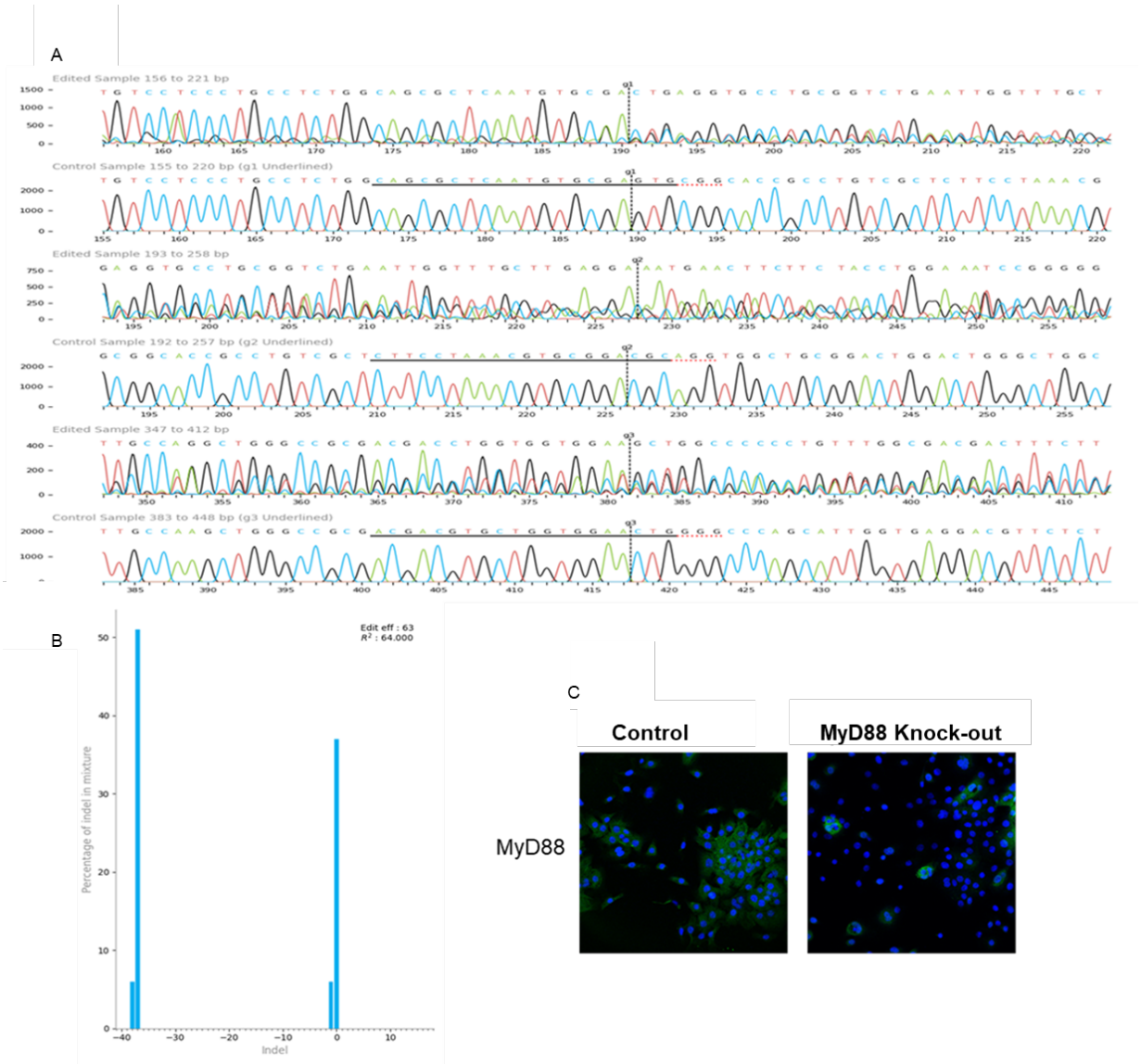


Fig. S6. Validation of MYD88 knockout in CRISPR/Cas9-edited T3 cells.ICE analysis of Sanger sequencing traces obtained for the MYD88 locus in negative control and CRISPR/Cas9-edited T3 cells. Genomic DNA was amplified across the sgRNA target region and the PCR products were analyzed by Sanger sequencing at Eurofins Genomics. Sequence traces were analyzed using the Synthego ICE (Inference of CRISPR Edits) web tool. The negative control (Control) consisted of cells transfected with a non-targeting sgRNA designed not to recognize any genomic sequence. (A) Alignment of Sanger chromatograms covering the MYD88 sgRNA target site. In the negative control sample, the chromatogram remains clean and well resolved across the analyzed region, consistent with an unedited locus. In contrast, the edited sample shows overlapping and mixed peaks beginning at the expected Cas9 cleavage site and in the nearby surrounding sequences, indicating the presence of a heterogeneous population of alleles carrying insertions and deletions (indels) generated by CRISPR/Cas9 system. The black horizontal lines indicate the positions of the sgRNA target sequences (g1,

g2 and g3) within the MYD88 genomic region. (B) ICE-derived indel spectrum for the edited sample. The x-axis indicates indel size relative to the reference sequence, expressed in nucleotides, where negative values correspond to deletions. The y-axis represents the estimated proportion of each indel class within the cell population. ICE analysis estimated an overall editing efficiency of 63%, with a coefficient of determination ($R^2 = 0.64$). (C) Immunofluorescence staining of MYD88 in control and MYD88-KO T3 cells. MYD88-KO cells show markedly reduced MYD88 expression, confirming successful gene disruption. Green, anti-MYD88; blue, DAPI.

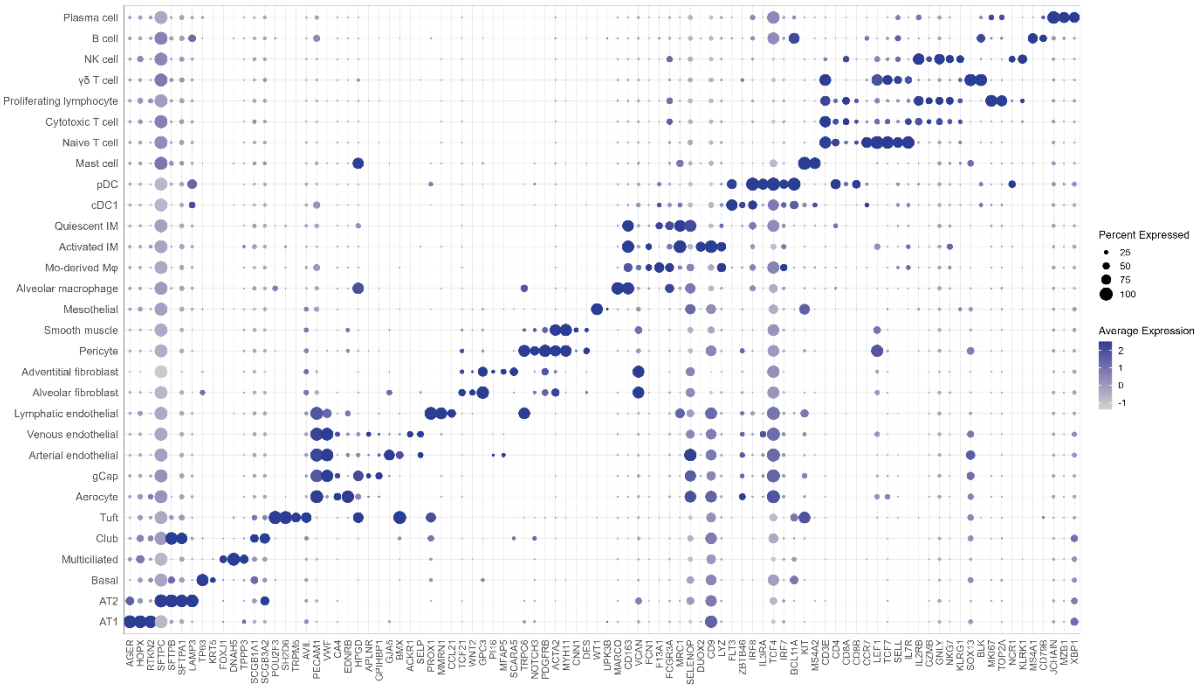


Fig. S7. Dot plot visualization of single-nucleus RNA-seq clusters displaying expression of canonical cell type marker genes. Dot size reflects the percentage of cells within each cluster expressing a given gene; dot color reflects the scaled average expression level.

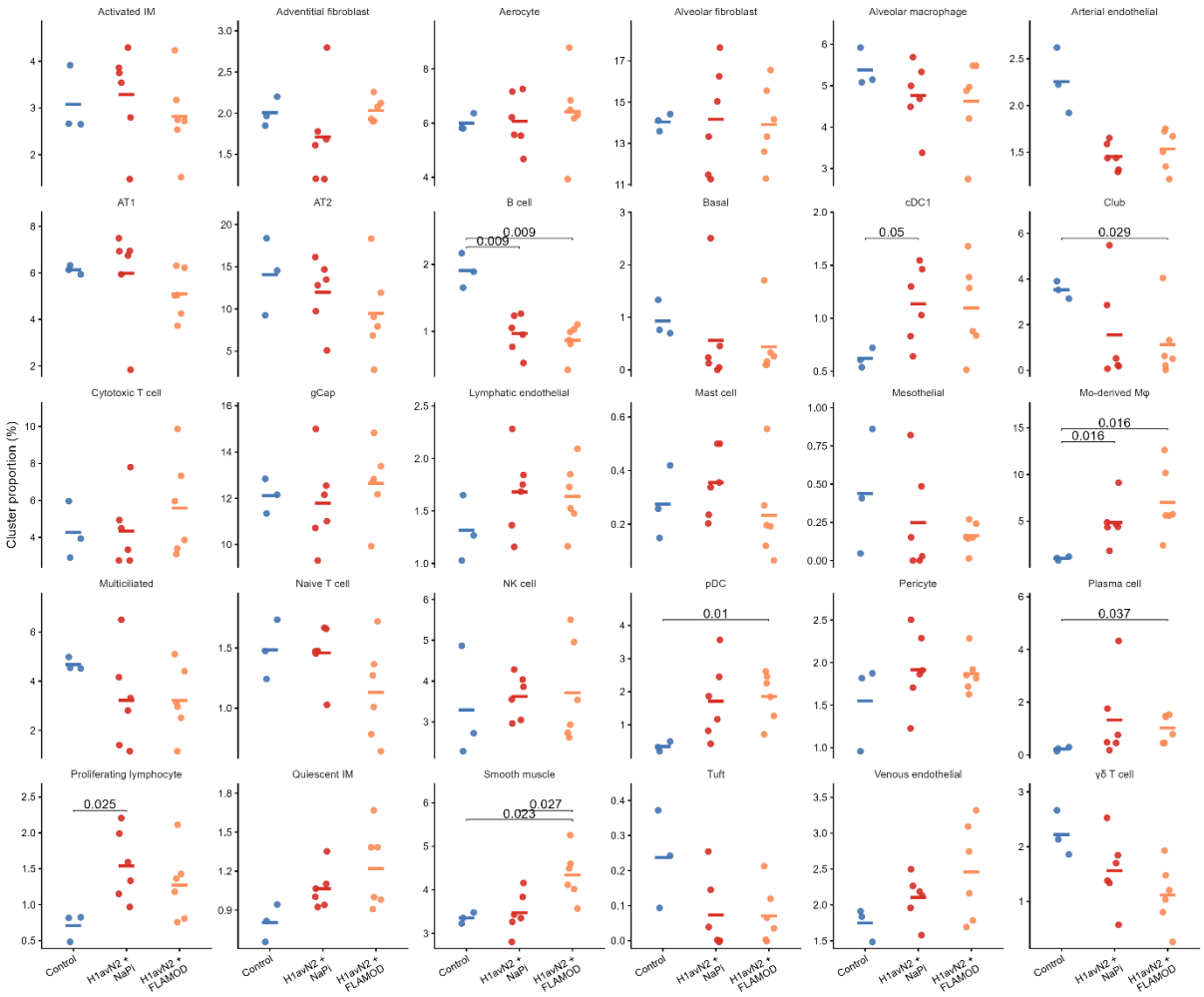


Fig. S8. Cell type cluster proportions across experimental groups. Each dot represents an individual animal (n per group as shown). Horizontal bars indicate group means. Cluster proportions were calculated as the percentage of each cell type relative to total recovered nuclei per sample. Pairwise comparisons between groups were performed usingvt-tests with Benjamini–Hochberg correction for multiple comparisons; adjusted p-values are shown only for significant contrasts (p.adj < 0.05).

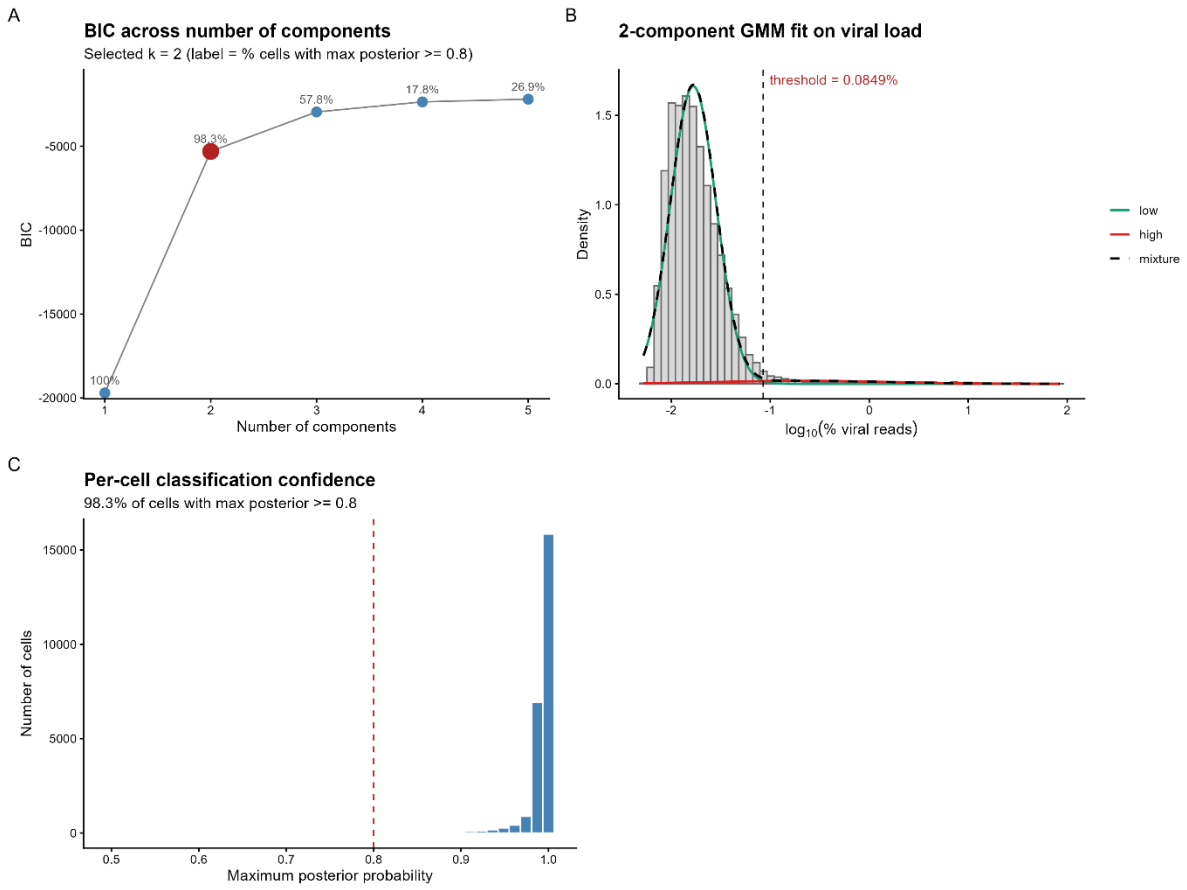


Fig. S9. Gaussian mixture model–based classification of viral load in infected cells. (A) Bayesian Information Criterion (BIC) across mixture models with k = 1 to 5 Gaussian components fitted to $\log_{10}$-transformed viral read percentages. The selected two-component model (k = 2, red) provided the best balance between model fit and classification confidence. Labels above each point indicate the percentage of cells classified with maximum posterior probability ≥ 0.8. (B) Two-component Gaussian mixture model fit to the $\log_{10}$ distribution of viral read percentages in infected cells. Green and red curves represent the "low" and "high" viral load components, respectively; the dashed black curve shows the combined mixture density. The vertical dashed line marks the GMM-derived classification threshold (0.0894% viral reads) at which posterior probabilities of the two components intersect. (C) Distribution of maximum posterior probabilities across single cells. The dashed red line indicates the 0.8 confidence threshold; the proportion of cells classified above this threshold is reported in the subtitle. Based on this classification, cells were assigned to one of four infection states: control (uninfected animals), bystander (infected animals, no detectable viral reads), low, or high viral load.

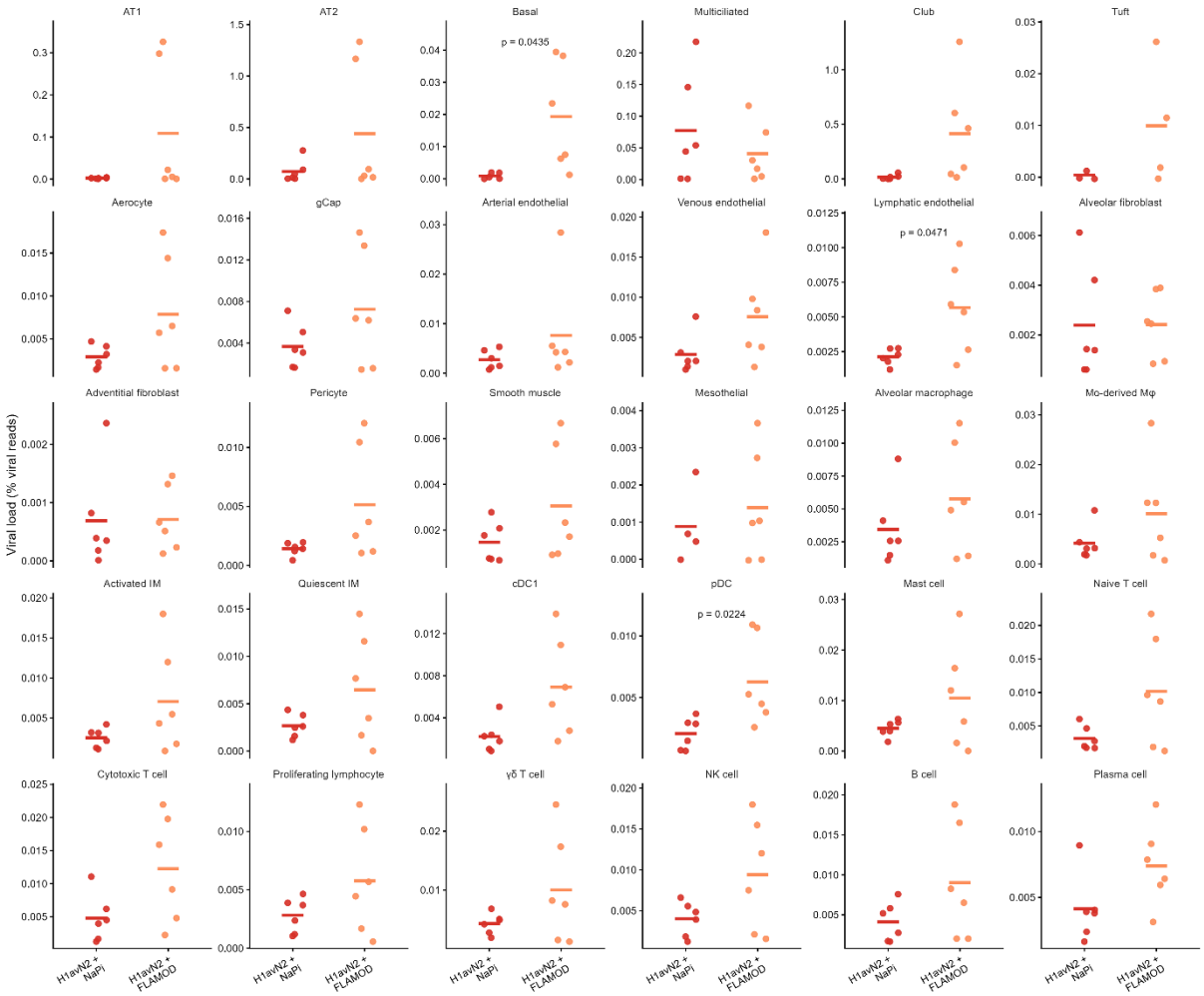


Fig. S10. Viral load per cell type cluster across H1avN2-infected groups. Each dot represents the mean percentage of viral reads per animal (n = 6 per group). Horizontal bars indicate group means. Pairwise comparisons between H1avN2 + NaPi and H1avN2 + FLAMOD were performed using Wilcoxon rank-sum tests for clusters violating normality (Shapiro-Wilk, $p < 0.05$) and Student's or Welch's t-tests otherwise, based on Levene's test for equality of variances. P values are shown only for significant comparisons ($p < 0.05$).

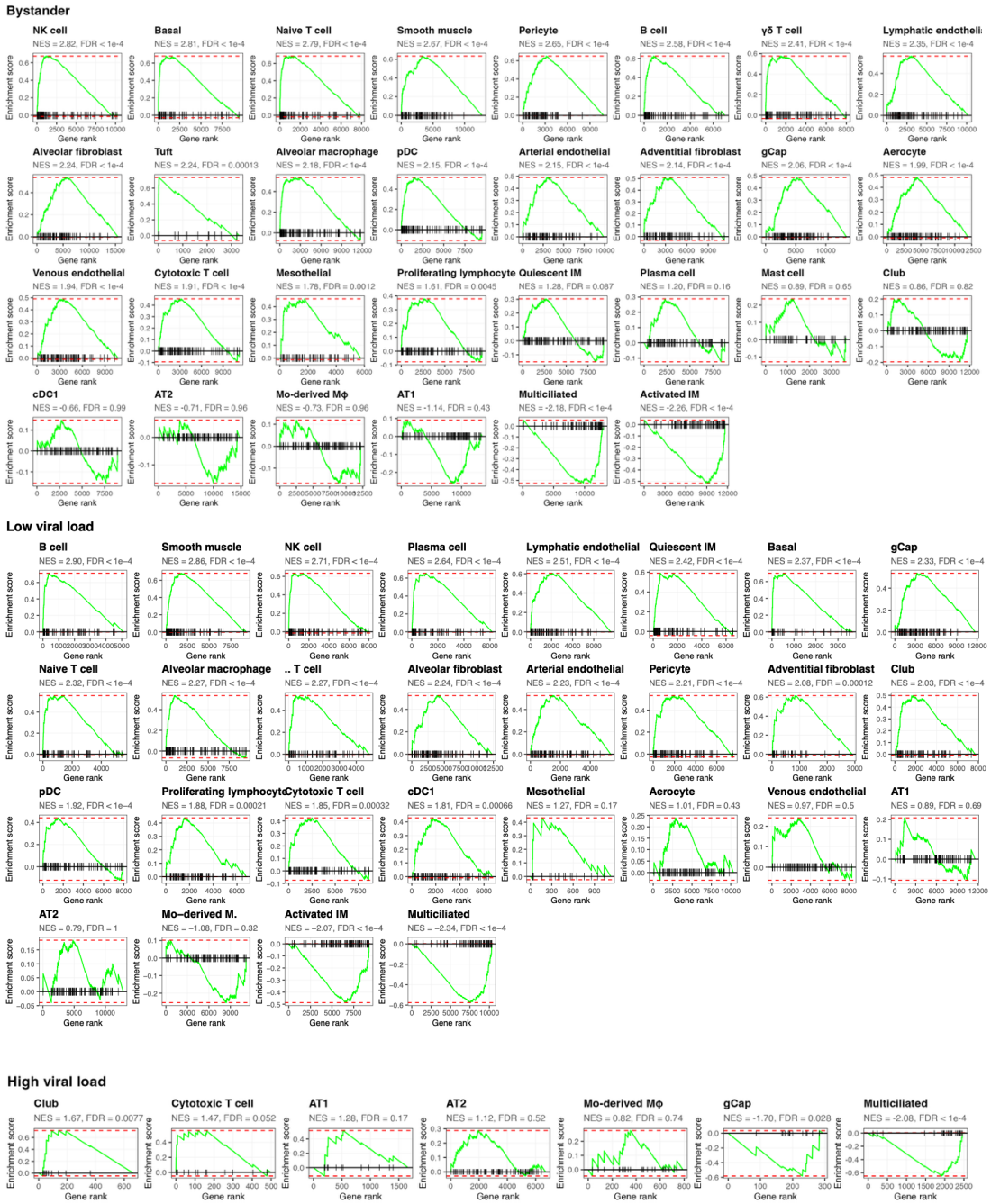


Fig. S11. GSEA enrichment curves across lung cell types, Type I IFN-induced ISGs. Each panel shows the GSEA running-sum curve for FLAMOD vs NaPi in one cell type, with the position of Hallmark Type I ISGs gene set members indicated by ticks below each curve. NES = normalized enrichment score; FDR = Benjamini-Hochberg-adjusted p-value. Cell types are ordered by NES.

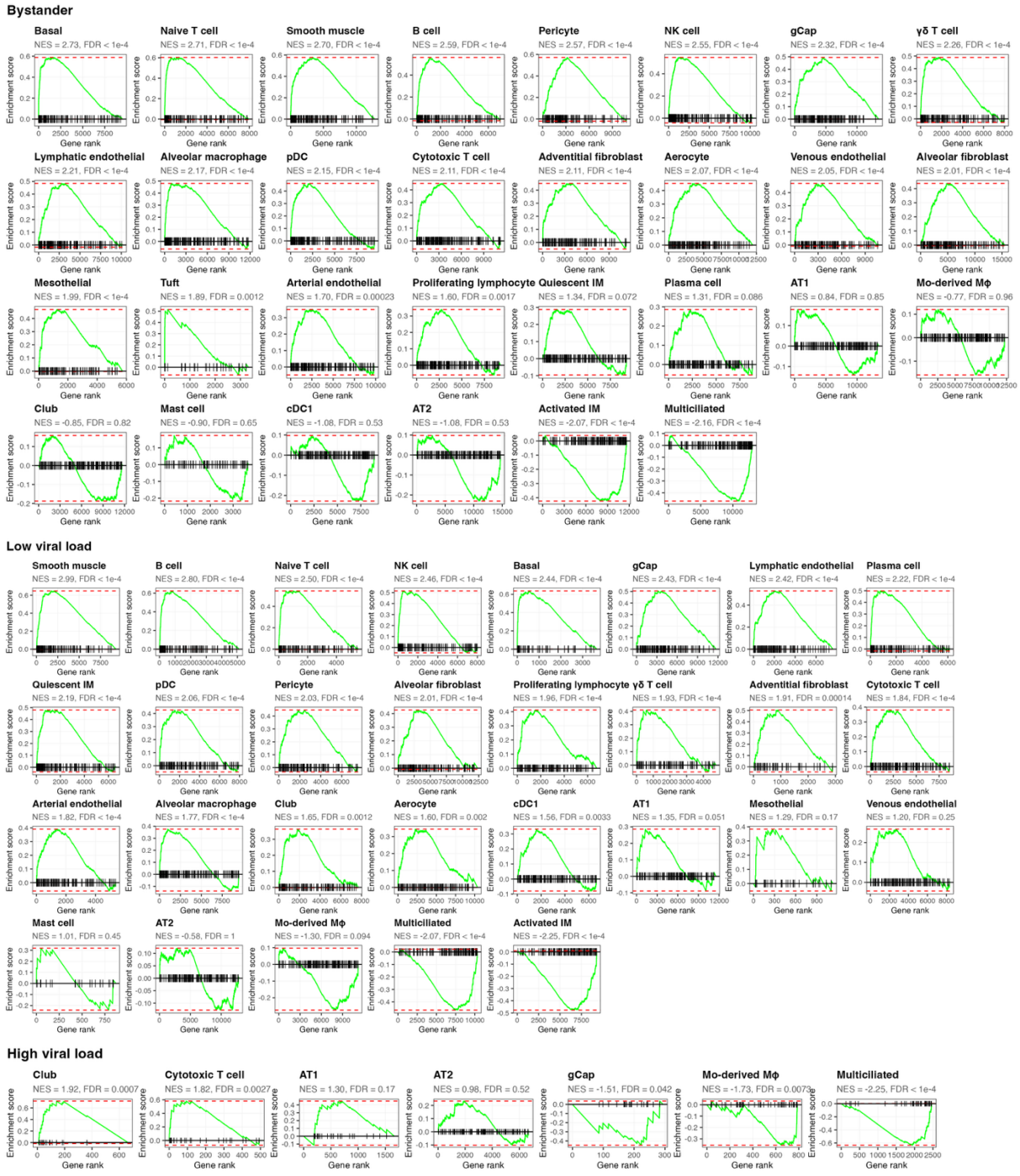


Fig. S12. GSEA enrichment curves across lung cell types, Type II IFN-induced ISGs. Each panel shows the GSEA running-sum curve for FLAMOD vs NaPi in one cell type, with the position of Hallmark Type II ISGs gene set members indicated by ticks below each curve. NES = normalized enrichment score; FDR = Benjamini-Hochberg-adjusted p-value. Cell types are ordered by NES.

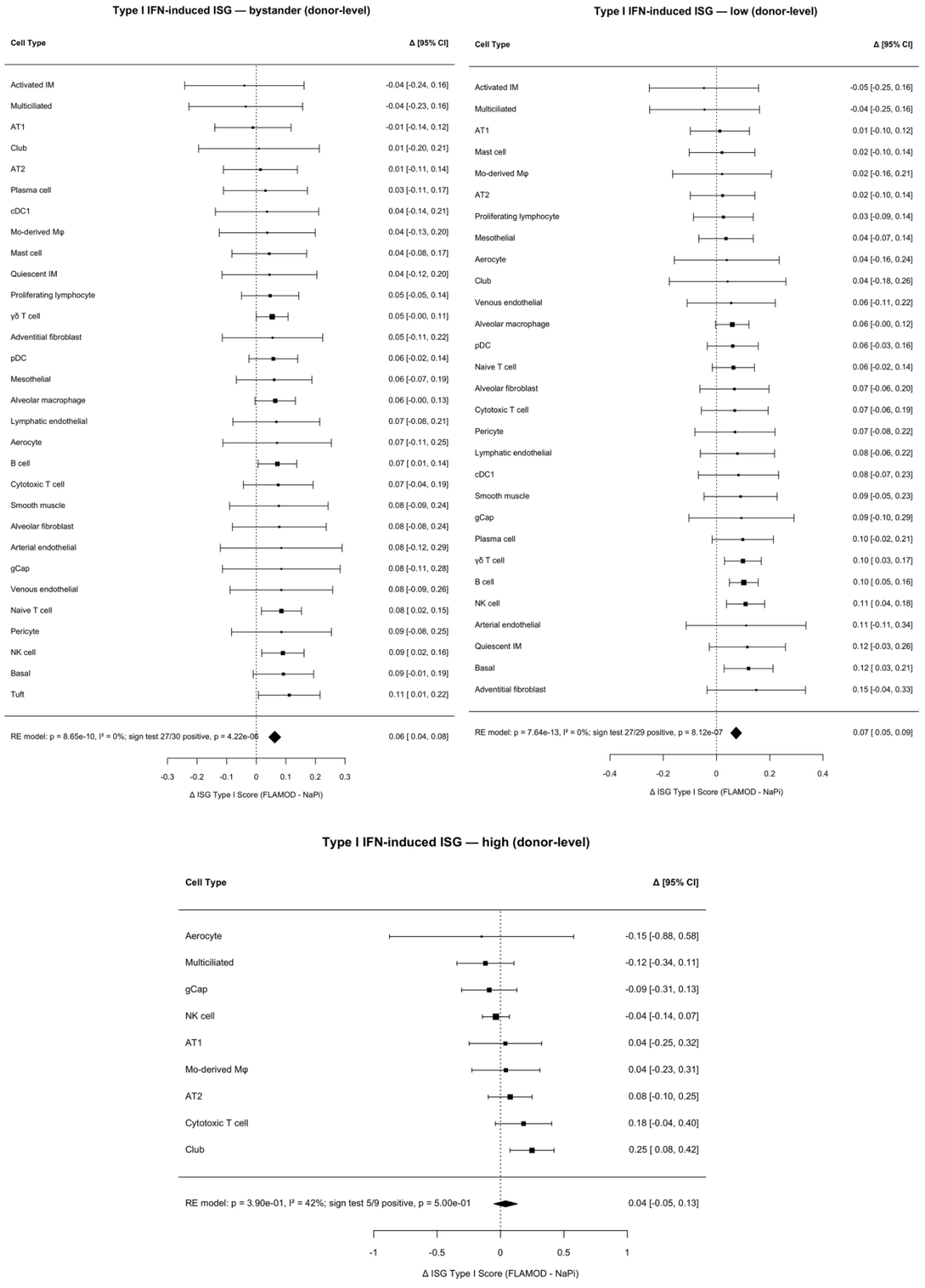


Fig. S13. Type I IFN-induced ISG scores forest plots. Random-effects meta-analysis of Type I ISG score differences (FLAMOD − NaPi) across cell types, stratified by infection state. Each row represents one cell type; squares indicate

the mean effect size and horizontal lines the 95% confidence interval. The pooled estimate (diamond) is derived from REML random-effects modelling.

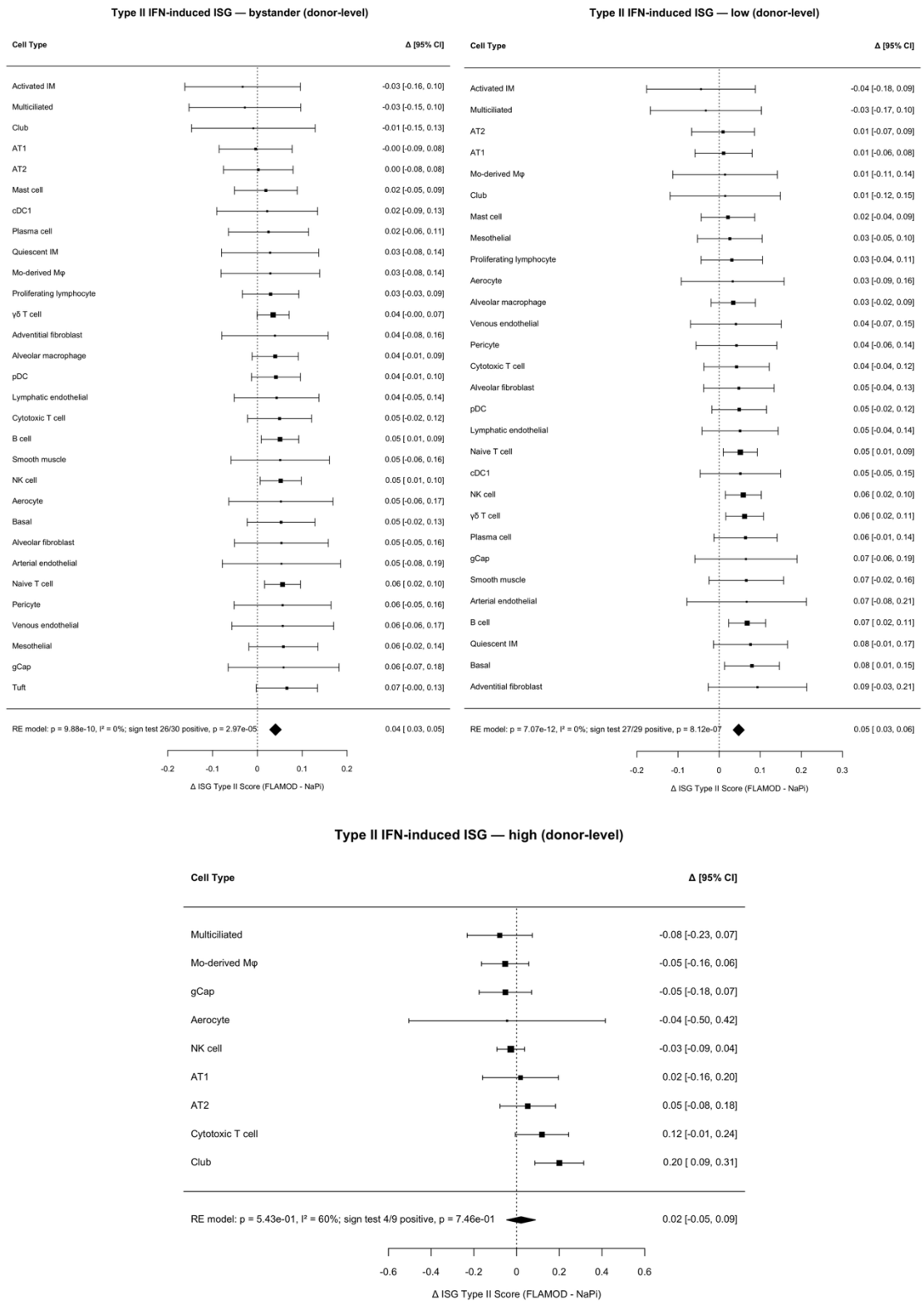
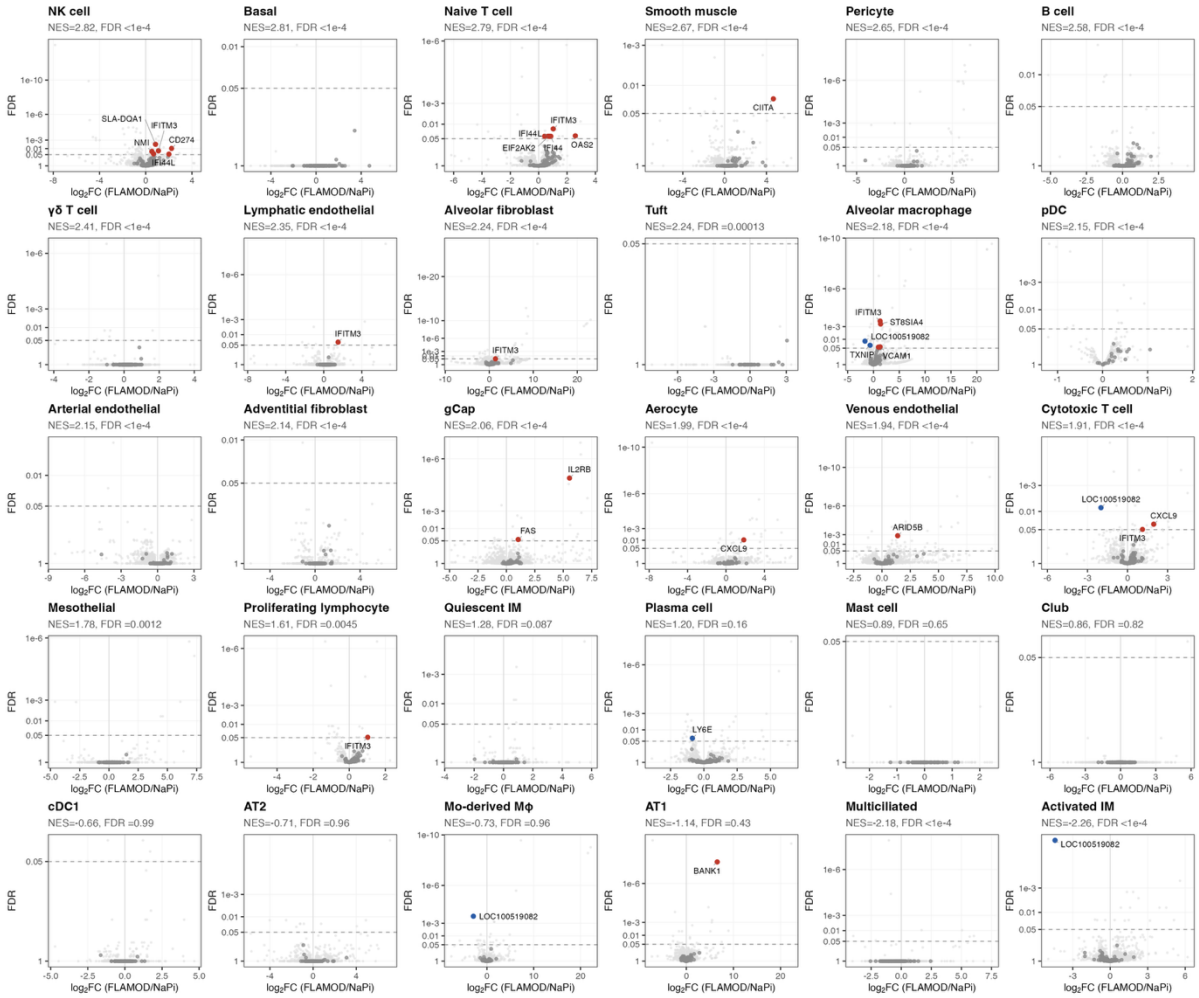


Fig. S14. Type I IFN-induced ISG score forest plots. Random-effects meta-analysis of Type I ISG score differences (FLAMOD − NaPi) across cell types, stratified by infection state. Each row represents one cell type; squares indicate

the mean effect size and horizontal lines the 95% confidence interval. The pooled estimate (diamond) is derived from REML random-effects modelling.

FLAMOD vs NaPi differential expression — Bystander, all cell types

Red = significantly upregulated ISG (FDR<0.05); blue = significantly downregulated ISG; grey = non-significant ISG; light grey = non-ISG. Dashed line: FDR=0.05.



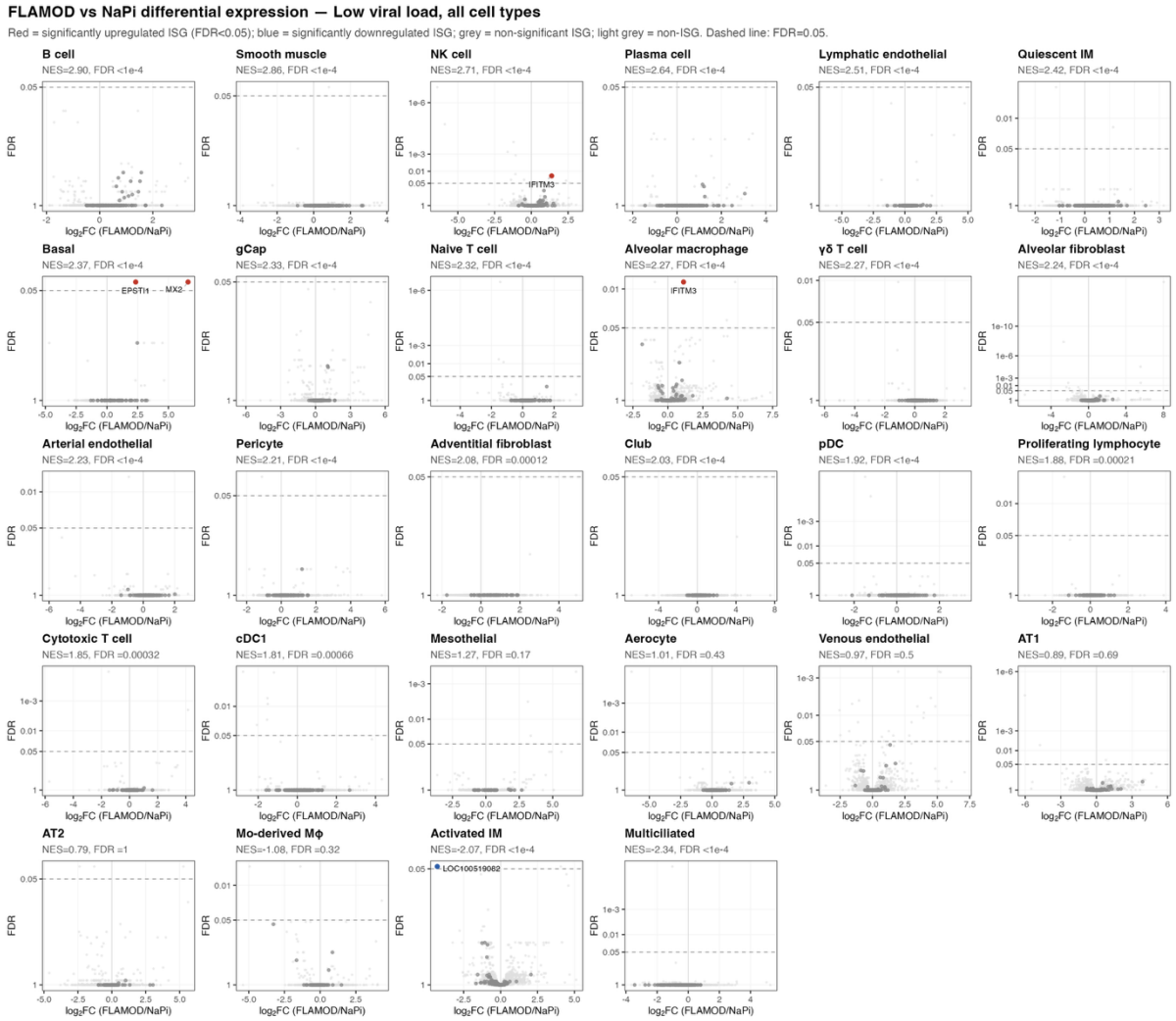


Fig. S15. Volcano plots of differentially expressed ISGs between FLAMOD and NaPi in bystander and cells with low viral loads in selected cell types. Red and blue dots indicate genes significantly upregulated and downregulated in FLAMOD-treated animals, respectively (FDR < 0.05). Dark grey indicates non-significant ISGs. Light grey indicates non-ISG genes. Gene labels are shown for significant genes only. Statistical significance was assessed by DESeq2 Wald test on pseudobulk counts (FLAMOD vs NaPi); FDR is Benjamini-Hochberg-adjusted across all genes per cell type.

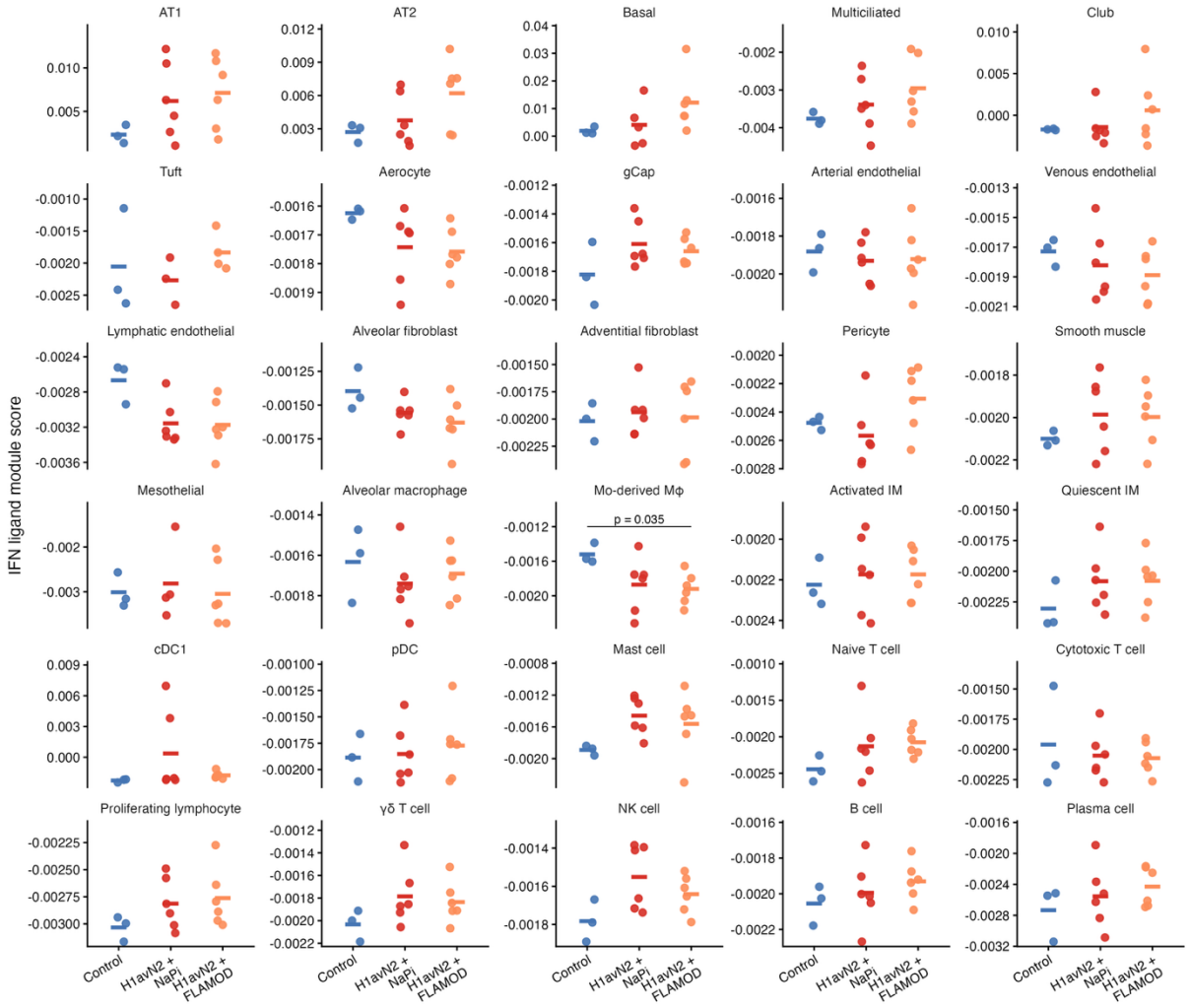


Fig. S16. Type I IFN expression across cell types and correlation to ISG response. (A) Type I IFN module score per cell type cluster across treatment groups. Each dot represents the mean module score per animal (n = 6 per group). Horizontal bars indicate group means. The module score was computed from a curated panel of pig Type I IFN genes. Pairwise comparisons between Control, H1avN2 + NaPi, and H1avN2 + FLAMOD were performed using Wilcoxon rank-sum tests for clusters violating normality and Student's or Welch's t-tests otherwise, based on Levene's test for equality of variances. P values were adjusted for multiple testing by the Holm method. (B) Per-pig correlation between mean Type I IFN module score and mean Type I (left) or Type II (right) ISG module score, computed across all cells per animal. Each dot represents one pig, colored by treatment. The grey line and shaded ribbon show the linear regression fit with 95% confidence interval. Spearman correlation coefficients (ρ) and associated p values are indicated.

Table S1. Primers used for evaluation of gene expression by real-time quantitative PCR amplification. Tm for all primer couples was 60°C.

Gene	Forward primer	Reverse primer
AXL	TACTTCTGGGAGCAGTTGTGG	TCGAACACCTCTCCATAGCG
B2M	CGAGACCACTAACCGGCATCA	TGGATTCATCCAACCCAGATGCA
BANF	TGTTGTGTGCACTTCCAACG	GGGAGATGCATGCAAGTGTG
CASP3	AGCAGTTTTATTTGCGTGCTT	CAACAGGTCCATTTGTTCCA
CCL20	ACAGCAGCTCGCCAATGAA	GGATCTGCACACACGGCTAA
cGAS	AGGAAATCCTCTGGAACAGTTCTTA	CTCTCCACAGTGACACCTTCT
CSF2	TGCCATCAAAGAAGCCCTGA	GCATGTCGGCTCCTGGG
CXCL2	ATCCAGGACCTGAAGGTGAC	GGGTTGAGACAAACTTCCTGAC
CXCL8	TGCCTTCTTGGCAGTTTTCC	CTGCACTTACTCTTGCCAGAAC
DAI	GGGGTTTACCAGCCAGAAGA	GGAAATGCAGTTGTTCAGTCCC
DDIT3	GCTGAAGAGAACGAACGGCT	GGGAGTGCTGGTCCCAAAAG
DNAPKCS	CCCTGCTGGCAGGTGAG	CAGCCATGATCCGGTACGTT
EIF2AK2	GACTGGACCCTGCACTTCTA	CGACCACTGGCCATTTCTTT
GAPDH	CCTCAACGACCACTTCGTCAA	TGGTCCAGGGGCTCTTACT
HSP70.2	TGGTGAACCACTTCGTGGAG	AAGTCGATGCCCTCGAACAG
HSPA5	TAGCTTACGGTGCTGCTGTT	AGGGGTCGCTCACCTTCATA
IFI16	AGTCAGCATCCACAACTCTCA	GGGAGGCTACTGATCTTGGC
IFIT1	TGACTCACAGCAACCATGAGTAAT	TGTCTTGAATGACCAACTCCCA
IFNA1	GGCTCTGGTGCATGAGATGC	CAGCCAGGATGGAGTCCTCC
IFNAR1	TCAGTGGCTCCATGCCTTTT	GACACAATGGGTCGTTTTGACA
IFNGR1	CCATCAGATCCTCTCTGGGC	AGGGGGTCCAAATTTCCCTTG
IL18	TGTAGCTGAAAACGATGAAGACC	CGGCTTGATGTCCCTGGTTA
IL1A	TGTGCTAAATAACCTGGATGAGG	GGTTCGTCTTCGTTTTGAGC
IL4R	TGTCAGCACCTCTACCTGTGA	TCAGCATATGGCAGACGCAC
IRAK1	GTACCGGGCGGTGATGAGAA	TTGGGGTGACGAAACCGTGA
IRAK4	ATGGCACCTGAAGCTTTGCG	TGAGGTTCACGGTGTTCATCCA
IRF3	GCTACACCCTCTGGTTCTGC	GAGACACATGGGGACAACCT
ISG15	GGTGAGGAACGACAAGGGTC	CAGAACTGGTCAGCTTGCAC
KDM6B	CTCCCTACGGCTCAACTTGG	TGGAAGGAGGAAGCCTGGTA
MAP3K7	GGAGCAGTGTGGAGAGCTTG	ACGGTGGCCCCGTTTAGG
MAPK1	CCATCGCTGAAGCACCATTCA	CAGGAGCTGGGAGGAAGAACA
MAVS	GGACCTCTTCGACAGCCTTC	GCTGTTTGAATTCCGCAGCA
MCU	TGCAAGAAGAAGATCGGGGAA	TATCCCTGTTGAGGCAGCAA
MX1	AGTGTCGGCTGTTTACCAAG	TTCACAAACCCTGGCAACTC

MYD88	TGCGTCTGGTCCATTGCTA	TCAGAGACAACCACTACCATCC
NFKBIA	ATTCTGCAGGCCACCAACTA	AGACACCAACAGCTCCACAA
NFKB1	ATTCTGCAGGCCACCAACTA	AGACACCAACAGCTCCACAA
NFKBie	GCAGTTGGAAGCACTCACTT	GGAGTGCTGTCTGGTAAAGGT
NFKBiz	TTCGTGGATCTTGAGGCAACTA	CACAGCGTTGTGTGCCATAA
OAS1	ACACATGTTTCCGAACGCAG	AACTTGTGAGCTTGGTGAGGAAG
PBD1	ACCGCCTCCTCCTTGTATTC	CACAGGTGCCGATCTGTTTC
RAB1B	ACACCACGGCCAAGGAATTT	CAGCCATGGTCATGAACGC
RIG-I	CGACATTGCTCAGTGCAATC	TCAGCGTTAGCAGTCAGAAG
RPL19	GCTCAGAAGATACCGTGAATCTA	ACACATTCCCCTTCACTTTCA
RXFAP	ACACGTCAAACTGGAGGAAAGT	CTCTAAAAGAGTAGGTCTTGCAGGT
SAMHD1	TGTCTTGTTCGTGAACTGAGTGA	GAAAACGGCCCATGACCAAG
SIKE1	GCCCTTCCGGACCAGTATCAA	GCATCCTGGTGTTCCTCCAAG
SLFN11	TCCTACTCCATTCGCATCGC	CGTTACTCTCAGGACGCAGG
SOCS5	ACGCTGTGTTTGCAGTCTC	ACTTTCCAAGCTCCCTGTC
SOCS4	TCCTGGGACAGGCTCTATG	GGTACTTGGGAGGTGTTTC
SOD2	GGCCTACGTGAACAACCTGA	TGATTGATGTGGCCTCCACC
STAT2	CTCACTCTGGGGACCGGAAG	GCGCCATTTGGCCTCTGAAT
STIM1A	GCCTGGGATCTCAGAGGGAT	TTGGAAGGCATGGCACTGAA
STING	CCCAGCTGAAGTCTCTGCAA	TACGTTCTTGTGGCGTGAT
TBK1	TTTGAGAGATGTGGTGGGTGG	CATCTTCCCCTATCACACGCA
TGFB1	CTGGAAAGCGGCAACCAAAT	GCCCGAGAGAGCAATACAGG
TGFBR1	TGCTGCAATCAGGACCATTG	GCCAGATGGTGGCTTTCCTG
TGIF2	GCCGCTGGGAAAAGCTTGC	GCACTGACAGGTTGGTCTGT
TIMP1	CCCAGAGTTCAACCAGACCG	GATGAACCGGATGTCAGGGG
TLR3	CCTGCATTCCAGAAGTTGAG	TGAGGTGGAGTATTGCAGAG
TNFAIP3	AGGAAGCTTGTGGCACTGAA	TCCTGAACACCCCACATGTAC
TNFSF10	GGGCAGACCTGTGTGTTGAT	GGAGTACTTGTCCTGCATCTGT
UNC93B1	GCCGGACATCGACAGCAAAA	CGTGTAGTAGCGCTCCCAGT

Table S2. sgRNAs sequences for KO generation.

Gene	sgRNA 1	sgRNA 2	sgRNA 3
IFNAR 1	TCGAATGAAGATGAA AACAG	AGGAGAAGAAATTCT GCGAC	
MyD88	CAGCGCTCAATGTGC GAGTG	CTTCCTAAACGTGCG GACGC	ACGACGTGCTGGTG GAACTG
TRAF6	CAGCGTGATATGCTT CCCTA	CATCATTCTCATGTG CGACT	
Non-targeting control	AAAACAGGACGATGT GCGGC	AAAACATCGAAGCGT	AAAATAGCAGTAAAC TCAAC

Table S3. Primers used for sequencing of edited loci.

Gene	Forward PCR primer	Reverse PCR primer	Sequencing primer
IFNAR1	CCAACCCCAGCGAACCTCCAG	CACCGCAAGGCTATCGGCCG	CTCTCCACCTCTGAAGAACAAACCG
MyD88	GAGAGCTGAGACGGGGCGTCC	GCAGTCCCAAGTCCCCTACAGAG	GTAGGGCAGGGTGGCGCTTCTC
TRAF6	GTAAAAGAGACAGGGGGTAGCTAAGC	GTTTCTCCTCCTCTTGAGATTTCAAG	CTGATGAAGACAAAGAAGGTTGTGGGGG